Title

Spectroscopy of High-Temperature Systems

Author

Hicks, William T

Publication Date

1957-02-01

UCRL 3696

UNIVERSITY OF CALIFORNIA

Radiation Laboratory

BERKELEY, CALIFORNIA

DISCLAIMER

UCRL-3696

UNIVERSITY OF CALIFORNIA

Radiation Laboratory
Berkeley, California

Contract No. W-7405-eng-48

SPECTROSCOPY OF HIGH-TEMPERATURE SYSTEMS

William T. Hicks

(Thesis)

February 19, 1957

Printed for the U.S. Atomic Energy Commission

Contents

SPECTROSCOPY OF HIGH-TEMPERATURE SYSTEMS

William T. Hicks

Radiation Laboratory
University of California
Berkeley, California

February 19, 1957

ABSTRACT

The Swan and Phillips band systems of the C_2 molecule were produced in emission in a source of thermal equilibrium. Measurements of the temperature coefficients of the intensities of these bands yielded values for the heats of formation of the $\underline{X}\ ^3\Pi_u$ and $\underline{a}\ ^1\Sigma_g^+$ states of C_2 from solid graphite. These measurements showed that the $^3\Pi_u$ state is 8 ± 4 kcal (0.35 ± 0.17 ev) lower than the $^1\Sigma_g^+$ state. Comparison of the results of this experiment with that of Krikorian[19] leads to 200 ± 5 kcal for the heat of formation of the $^3\Pi_u$ state from solid graphite at $0^\circ K$; this is probably the heat of sublimationof C_2 gas. The resulting D_0 of C_2 is 139.2 ± 4 kcal (6.04 ± 0.22 ev).

The position of some unobserved low-lying electronic states of C_2 are estimated by revising the predications of Mulliken.[24] Some of these states may be lower in energy than the $^3\Pi_u$ state. The discovery of infrared transitions between these states and some of the already observed states of C_2 would provide accurate relative energies for these states.

From absolute intensity measurements the absolute $\underline{f}$ value for the total Swan transition was determined as 0.03. The absolute $\underline{f}$ value measured for the Phillips (2-0) vibrational band was 4×10^{-3}. Both values are uncertain by a factor of two.

SPECTROSCOPY OF HIGH-TEMPERATURE SYSTEMS

INTRODUCTION

The purpose of this investigation is to find which of the electronic states of the C_2 molecule is the ground state. It has been commonly assumed for a number of years that the lowest of the triplet states, the $^3\Pi_u$ state, is the lowest state of the molecule. A number of strong transitions between singlet states have been observed, but unfortunately no transitions have been found between singlet and triplet states. The possibility that the lowest of the singlet states, the $^1\Sigma_g^+$ state, is the ground state has not yet been ruled out.

Basing their work on the assumption that the $^3\Pi_u$ state is the lowest state of C_2, two workers have tried to determine the heat of formation of C_2 vapor from solid graphite by spectroscopic methods. Brewer, Gilles, and Jenkins[1] observed the intensity of the (0-0) Swan band ($^3\Pi_g \rightarrow {}^3\Pi_u$) in emission as a function of temperature. They produced the C_2 in a King furnace (a carbon-tube resistance furnace) at temperatures of from 2700 to 2900°K. and observed the band through a small glass prism spectrograph by a photographic technique. If one assumes that the intensity of the transition is directly proportional to the concentration of molecules in the particular state from which the transition arises, then by the second law of thermodynamics a plot of $R \ln IT$ versus $1/T$ will have as its slope ΔH^*_T, which is the heat for the reaction

$$2C \text{ (graphite)} = C_2^* \text{ (gas in the excited state)}. \qquad (1)$$

Here T is the absolute temperature at which the intensity I is observed, and R is the universal gas constant. Knowing the excitation energy of C_2 and the heat capacities of solid graphite and the molecule, one may easily correct this heat to ΔH°_0 for the reaction

$$2C \text{ (graphite)} = C_2 \text{ (gas)}. \qquad (2)$$

Brewer, Gilles, and Jenkins obtained a heat for the reaction of 233.1 ± 7.0 kcal/mole.

This value has been questioned for several reasons. The slope method of determining the heat is never very accurate; usually the temperature range over which observations can be made spectroscopically is comparatively small, owing to self-absorption at the high temperatures and lack of sensitivity at the low temperatures. In addition, the accuracy of temperatures measured in the King furnace is limited by temperature gradients which develop in the carbon tube and which increase as the temperature is raised. These errors may make a heat uncertain by as much as 10%. The previous results are also poor because a photographic technique was used for the determination of intensities. The determination of light intensities by electronic techniques is much more precise than photographic methods.

There are at least two methods by which this heat might be determined more accurately. One is by the use of the third law of thermodynamics. One may obtain $(F^\circ - H_0^\circ)/T$ values for graphite up to 3000°K from the National Bureau of Standards Tables.[32] The $(F_T^\circ - H_0^\circ)/T$ values for C_2 gas. may also be calculated if the electronic, vibrational, and rotational energy levels of C_2 are known. The difference in these values gives $(\Delta F_T^\circ - \Delta H_0^\circ)/T$ for Reaction (2). Now if we knew the absolute absorption coefficient for the Swan transition, from the measurement of the absolute intensity of the band we could compute the actual concentration of the C_2 gas. Since

$$\frac{\Delta F_T^\circ}{T} = - R \ln p_{C_2} , \qquad (3)$$

we may calculate $\Delta F_T^\circ/T$ and subtract it from the above function for Reaction (2), thus obtaining $-\Delta H_0^\circ/T$. This method obviates the error in temperature measurement in the slope method. Here the error in temperature appears but once, and only in the absolute value. In the slope method two temperature errors are made; then the error is badly compounded by taking a small difference between two large numbers.

Since in the case of the Swan bands and the spectra of most other diatomic molecules accurate absorption coefficients have not been measured, this method is not yet available to us. However, there is a way in which we may use the slope method to better advantage. Let us measure the comparatively small difference in energy between the unknown heat and one which is known accurately. The error arising from temperature measurement in any heat measured over a given temperature interval will always be a certain percentage of that heat. Thus the absolute error in the small energy difference will be smaller than the error in the unknown heat measured by itself.

This was the method employed by Krikorian in measuring the heat of formation of the $^3\Pi_u$ state of C_2 gas from solid graphite. To provide a known heat he used the element zirconium, which has a spectral line at 4739.48 A near the (1-0) Swan band head at 4737.1 A. He heated the zirconium metal in the graphite tube of a King furnace and allowed it to become carburized. Then using a photomultiplier, he traced through both emission spectra with the gases at a constant temperature, and repeated the tracing at different temperatures. From the data thus obtained he was able to make a plot of $-R\ell n(I_{Zr}/I_{C_2})$ versus $1/T$. From the slope of this plot he obtained the difference in the heat needed to vaporize one mole of C_2 from solid graphite to the gas in its excited state and the heat needed to elevate one mole of zirconium from solid ZrC and C to a mole of zirconium gas in its excited state. Krikorian thus obtained a heat for the $^3\Pi_u$ state of C_2 of 191.4 ± 5 kcal per mole.

Mass-spectrographic evidence seems to point to a value for the heat of sublimation of C_2 gas at the upper end of this range. Honig,[15] using a slope method, obtained a value of 199 ± 20 kcal per mole for ΔH^o_{2400}. From this one may obtain ΔH^o_0 = 202 ± 20 kcal, using the heat capacity data for C_2 gas given by Stull and Sinke[35] and those for graphite given by the Bureau of Standards.[32] Chupka and Inghram[5] obtain ΔH^o_0 = 183 ± 10 kcal by a second-law experiment. On the other hand, by estimating the ratios of the cross sections of C_1 and C_2 to that of silver, with which they calibrated their apparatus, they

could calculate vapor pressures of C_1 and C_2. Then, using the third law, they obtained ΔH_0^o = 170 ± 7 kcal per mole for C and ΔH_0^o = 197 ± 7 kcal per mole for C_2. They point out that the value they obtained by the second law may be too low, owing to vaporization of magnesium from their apparatus at the lower end of their temperature range.

In Krikorian's work and other work done by optical spectroscopic methods, the heat that is measured for the formation of the $^3\Pi_u$ state is the heat of vaporization of the C_2 molecule only if this state is the ground state of the C_2 molecule. The mass-spectrographic methods using the second law do not depend at all on which is the lowest state of the molecule. However, if the third law is used, then entropies or $(F^o - H_0^o)/T$ values for the C_2 molecule must be calculated from optical spectroscopic data, and this again involves knowing the nature of the ground state of this molecule.

Thus the idea for this investigation arose, i.e., to determine which of the two observed states, $^3\Pi_u$ or $^1\Sigma_g^+$, may be the ground state of the C_2 molecule. Suppose one produces both the Swan spectrum and one of the singlet-state transitions at the same time, using an equilibrium thermal source such as the King furnace. Then one can observe how the ratio of the intensities of the two spectra changes as a function of temperature. Thus one obtains the difference in energy between the two states from which the transitions originate, much as Krikorian did with zirconium and the Swan bands. It may be pointed out that this situation is even more favorable than that of Krikorian's. Both transitions arise in the same molecule, and even if the molecules are present at somewhat less than equilibrium pressure, one can still obtain a true energy difference by the slope method as long as the ratios of molecules in the various states still have equilibrium thermal distribution. Since the singlet states of C_2 are all interrelated by transitions, the energy difference between any singlet state and a triplet state yields the energy difference between the $^3\Pi_u$ state and the lowest singlet state, $^1\Sigma_g^+$.

Now let us investigate the singlet-state transitions of C_2 to see which one will best suit our purpose. Four singlet transitions have been reported for C_2.[31,11] These are the Deslandres-Azambuja, the Mulliken, the Phillips, and, the most recently discovered, the Freymark systems. The electronic states of both the Deslandres-Azambuja system ($c\,^1\Pi_g$ - $b\,^1\Pi_u$) from 3400 to 4100 A and of the Freymark system ($b\,^1\Pi_u$ - $e\,^1\Sigma_g^+$) at about 2200 A are too highly excited to permit the finding of their transitions either in emission or absorption in a thermal source at temperatures such as the King furnace produces. The Mulliken bands ($d\,^1\Sigma_u^+$ to $a\,^1\Sigma_g^+$), appearing at about 2300 A, have an upper state that is also too highly excited for the bands to be observed in emission in the King furnace. Their lower state, though, is low enough that they have been reported in absorption in the King furnace by Brewer and Phillips,[2] who used a xenon high-pressure arc lamp as a source. However, because the rotational lines of these relatively headless bands were strongly self-absorbed, and because of the usual difficulties of working this far in the ultraviolet, it was decided that the Phillips bands might be a better system to use for this purpose.

Accordingly the investigation reported here began with a search for the emission spectrum of the Phillips bands in the King furnace. It was described by Phillips as a transition between the $b\,^1\Pi_u$ and the $a\,^1\Sigma_g^+$ states of C_2, and he reported its appearance at from 7900 to 9000 A in a discharge tube through which he streamed argon and benzene vapor.[25] In the present search the spectrum of the King furnace was produced by sending its emitted radiation into a three-meter diffraction-grating spectrograph. This spectrum was scanned with a cesium oxide phototube as detector. The (2-0) and (3-1) bands of the Phillips system were uncovered in this manner with furnace temperatures as low as 2710°K. These are the strongest bands that one might expect to find in the King furnace, since bands of lower vibrational quantum number are located too far in the infrared to be detected by the cesium oxide phototube.

The decision remained whether to compare the intensities of the triplet and singlet systems in absorption or emission. The greater the energy difference being measured the greater is the uncertainty in the determination, if measurement of temperatures is the main source of error. Therefore, if all other things are equal, whether absorption or emission is more accurate depends on whether the two upper or the two lower vibrational levels of the $^3\Pi_u$ and the $^1\Sigma_g^+$ states are closer. This in turn depends on the relative excitations of the singlet and triplet systems and the particular vibrational bands of the systems one uses. How the particular vibrational bands of the Phillips and Swan systems used in this experiment were chosen is discussed in a later section of this paper. Since the relative excitation energy of the singlet system was not know beforehand, an emission experiment was tried, as it is by far the simpler experiment.

EXPERIMENTAL EQUIPMENT

The King furnace used in this research was the same as that used by Krikorian[19] and very similar to the one described by Brewer, Gilles, and Jenkins.[1] The most important element of the furnace is a hollow graphite resistance heating tube, which is 12.5 inches long. The symmetrical tube has a one-half inch bore down the center and an outside diameter of 7/8 inch at the ends and middle. The wall is 3/16 inch thick in the middle of the tube and is then tapered symmetrically down to 1/16 inch at points 3-1/4 inches from the ends, where the thickness suddenly increases to 3/16 inch. This provides a uniform heating zone of 6 inches, bordered on each end by a sharp temperature gradient. The purpose of the tapering is to counteract the flow of heat out of the open ends of the heating zone by increasing the power output of the walls in these regions. Small, striated baffles, with 1/8-inch holes bored through them, are placed inside the tube just at the end of the uniform heating zone to help increase the temperature and pressure gradients.

The heating tubes are supported by two flexible graphite bushings which are tightly fitted into insulated copper blocks; these are in turn connected to copper bus bars which lead to a transformer. Also supported by the copper structure is a spool-shaped piece of graphite, which encircles the tube and holds five layers of concentric, cylindrical graphite radiation shielding. This whole structure is surrounded by a large brass barrel which has quartz windows opposite the ends of the heating tube. Copper tubing is provided throughout the entire structure to provide water cooling of the metal parts. The system is provided with vacuumtight seals so that it may be evacuated to pressures on the order of a micron.

The source of power is a 440-volt 90-ampere 60-cycle line. This is led into a 100-kva transformer capable of reducing the 440 volts down to 30 or any of a number of lower voltages, depending on which contacts on the transformer are used. Normal operating currents are of the order of 1500 to 2000 amperes with voltages of 10 to 15 volts. A fine adjustment on the power supplied to the furnace is provided by an internal auxiliary circuit controlled by a Powerstat.

This arrangement is capable of producing temperatures of more than 2800°C throughout the heating zone. The temperatures attained are limited only by the nonuniform vaporization of the heating tube. This produces large temperature gradients that cause the tube to fracture and break the electrical circuit. The temperature limit could be raised by use of a heating element made of TaC; however, such a tube would be more difficult to fabricate. The temperatures were measured by the use of a Leeds and Northrup Optical Pyrometer sighted through the window onto the walls of the heating tube.

The light from the King furnace is focused on the slit of a 3-m grating spectrograph. The spectrograph, scanning equipment, amplifier, and recorder are the same as those used by Krikorian.[19] The photometric equipment was built by Phillips[27] and described by him. The concave grating has 15,000 lines per inch ruled on its face, and a dispersion of about 5 A per millimeter in the first order. Because of its Eagle mounting, only about a 1600-A range is available in the first order with any one setting of the plate tilt, grating, and slit. The cesium oxide phototube is mounted in a scanning device on the Rowland circle of this spectrograph. The speed of the scanning device can be adjusted from about 0.67 A to 85 A per minute in the first order by using different gear trains. The signal from the phototube and its preamplifier is led into the amplifier, which when in use with this cell has an amplification variable by a factor of ten.

The Cs_2O phototube was of the type CE 25 A/B manufactured by the Consolidated Engineering Company of Geneva, Illinois. Though its sensitivity in the visible region of the spectrum is not as good as a 1P21 photomultiplier, a Cs_2O type tube is the best receiver for the region of the Phillips bands. The cell with its preamplifier circuit is contained in a small brass drum which is capable of being evacuated; electrical connections lead from this drum to the amplifier and recorder. In the preamplifier circuit the plate current of the phototube, is lead through a Hi-Meg resistance (10^{13} ohms). The voltage drop across this resistance controls a tetrode whose plate current is received by

the aforementioned amplifier. This whole circuit must be kept at a pressure of less than 0.1mm of mercury to prevent the condensation of moisture on the surfaces of the circuit.

With the previously existing equipment the signal-to-noise ratio of the photometric circuit was too low for an adequate study of the variation of intensity of the Phillips bands from low to high temperatures. Therefore it was decided that the phototube would have to be cooled to dry ice temperatures. Refrigeration has in similar systems produced considerable improvement in sensitivity; furthermore the use of liquid nitrogen has no advantage over cooling with dry ice. In order to cool the system and at the same time evacuate the circuit it was found necessary to make a few changes in the construction of the drum. The base of the drum through which leads ran to the power supply and amplifier had been sealed to the drum by means of a rubber O ring compressed by screws. It was found that when the drum was cooled the O ring contracted, became hard, and no longer held a vacuum. This seal was then replaced with a flat gasket made of soft aluminum. The gasket is clamped between a flat surface on the base of the drum and a boss of about 1/32-inch radius machined on the edge of the upper portion of the drum. The boss sinks into the soft gasket and produces a vacuumtight seal even if there are minor scratches on the face of the gasket. This seal remains vacuumtight when cooled, since the aluminum does not contract as much as the rubber at dry ice temperatures.

Difficulty was also encountered with the window in the drum; light from the diffraction grating passes through this window and falls on the photosensitive surface of the Cs_2O cell. This pyrex disc had originally been sealed to the face of the brass drum through the use of a second rubber O ring; this seal also failed when the drum was cooled. After several unsuccessful attempts to seal the glass window to the brass, it was found that Araldite, a thermosetting resin, produced a vacuumtight seal which remained leaktight when the system was cooled to dry ice temperatures. A form of Araldite which sets at room temperature with the aid of a catalyst worked best in this case because of the soldered joints in the drum.

After these corrections were made it was found that an approximately eightfold increase had been made in the signal-to-noise ratio as a result of cooling the cell to dry ice temperatures. In addition, Prof. F.A. Jenkins found that the diffraction grating had not been installed properly. He turned it over and realigned it so that its effective blaze angle of about 8000 A could be used. This improved the signal by a factor of about five. These improvements in signal-to-noise ratio permitted the Phillips system of the C_2 molecule to be observed in the King furnace to a temperature 150^{o} lower than in the preliminary measurements. This amounted to a considerable increase in the range over which intensity measurements could be taken.

EXPERIMENTAL PROCEDURE

Selection of Features to be Measured

For the purpose of rapid simultaneous scanning, Swan bands were needed that could be scanned along with the strongest Phillips band without having to change the position or range of the 3-m grating. The (0-0) and (1-0) Swan-band heads are so located that their second-order spectra and the first-order spectrum of the (2-0) Phillips band may be observed without changing the setting of the spectrograph. These are two of the strongest Swan bands in the spectrum of the King furnace; their heads are located at 5165.2 and 4737.1 A, respectively.

The Swan bands are made up of closely spaced rotational lines, which form well-defined heads. Therefore the intensities of the heads of these bands were measured above a background which consisted of scattered light from the furnace. The wave lengths of these band heads were checked in the finding lists of Moore[22] and the atlas of Rosen[31] to find impurity spectra that might occur in the King furnace. If impurities existed with spectra at just these wave lengths, they would have different heats of vaporization than the C_2 molecule and would therefore affect the measured heat according to how much they contributed to the spectrum under observation.

Multiplet four of the metal titanium is located near the Swan (0-0) band, but none of these lines is within an instrumental half width of the head of this band. The instrumental half width is determined by the slit width and scanning speed used in the experiment. Therefore this multiplet cannot contribute to the intensity of the (0-0) band head as measured here. Also, there are no atomic multiplet groups near the (1-0) Swan band that might contribute to the measured intensity of that head. An examination of Rosen's atlas also showed that there are no spectra from diatomic molecules that could be expected to appear in the King furnace and interfere with intensity measurements of either of these heads.

The Phillips bands are quite different in structure from the Swan bands; they consist of single rotational lines which are widely spread and which therefore form heads of weak or only moderate intensity. In fact many of the individual lines have greater intensities than the heads. For this reason it was decided to use a single rotational line of a Phillips band for the intensity study. The strongest band of this system that can be observed in the King furnace is the (2-0) band; its head is at 8751 A, and it is degraded to the red. The strongest branch of the Phillips bands is the Q branch. In the (2-0) band the lines of this branch gradually increase in intensity as we go to the red until we come to the line nearest the location of the head of the (3-1) Phillips band at 8980.5 A. Here there is an abrupt increase in intensity due to the superposition of some of the lines of the (3-1) head on the (2-0) rotational line at this wave length. Thus for the intensity measurements the last line in the Q branch of the (2-0) band that is clear of the (3-1) head was used. The heat that we then obtain from measuring the temperature coefficient of this line intensity is simply the heat of formation of this particular rotational level in the $v' = 2$ vibrational state. There is no contribution from a line in the (3-1) band that would yield a higher heat corresponding to the heat of a particular rotational level of the $v' = 3$ vibrational level.

The particular line we finally choose, therefore, is the line with $J' = J'' = 32$, and is located at 8956.1 A. There is a line of the P branch of the (2-0) band with $J' = 25$ located at 8954.4 A which blends slightly with the above-mentioned line. However, the excitation energy of the rotational level that gives rise to this line is only 1828 calories below that of the line which we are to measure. Since this $J' = 25$ line contributes about 10% to the intensity that we measure, this blending lowers the heat measured by only 0.2 kcal. As we shall see, this is negligible compared with other errors involved in these measurements.

Again the Moore scanning list and the Rosen atlas were consulted for spectra of other molecules and atoms that might interfere with the measurement of the intensity of this line. No atomic lines that might cause difficulty were found near 8956.1 or 4478.1 A. A line at 4478.1 A

would interfere, since its second-order image would blend with the first-order image of the rotational line.

The red spectrum of the CN molecule does have some bands in this region. The (1-0) band shows up quite strongly in the King furnace; however, it is located at 9148.3 A and is degraded to the red. In addition the (2-0) CN band at 7876.4 A shows up, and there is some indication of the (3-1) band at 8067 A. It would appear that even without special attention the rotational structure of these bands diminishes to the extent that they would make a negligible contribution to the background intensity by the time we reach the head of the (2-0) Phillips C_2 band at 8751 A. However, special precautions insured that these CN bands contributed nothing to the measured intensities. The graphite tube, shields, and support used in the run were pumped out while the tube was heated for several minutes at a temperature of 2400°C. Then the inside of the furnace was flushed with argon and pumped out again to a pressure of 0.1mm. This removed much of the nitrogen that had been absorbed by the graphite from the air that entered the system when the heating tubes were changed. In addition, powdered zirconium was spread in the cooler ends of the heating tube to act as a getter for nitrogen. These measures reduced the CN pressure by a factor of two or three, as evidenced by the decrease in the intensity of the (1-0) CN band.

Measurement of Intensities

The experimental procedure used was comparatively simple. After the furnace had been pumped and flushed at low operating temperatures, enough argon was led in to produce a pressure of 1 cm of mercury when the argon was at room temperature. The purpose of the argon pressure was twofold. One function was to reduce the mean free path of thermal electrons so that they would not be accelerated down the heating tube by the 12-volt potential. Such accelerated electrons could excite the molecules that were being studied. Furthermore, the argon reduced the mean free path of the carbon atoms and molecules and prevented them from condensing on the quartz windows opposite the ends of the heating tube.

The next step was to adjust the Powerstat so that the furnace reached a temperature within the working range. This range was from about 2435°C to 2790°C. Below this range the features did not show up with certainty, and above this range gradients developed too rapidly in the heating tubes. In addition, the Swan features begin to suffer too much self-absorption above these temperatures. Time had to be allowed for the furnace to adjust to an even temperature after each adjustment of the Powerstat. The point at which the furnace had reached a constant temperature could be judged by taking successive readings on the walls of the tube with the pyrometer.

Then as rapidly as possible the scanning phototube was manually set slightly to one side of the location of one of the features, the scanning motor was started, and the feature was scanned. Then the phototube was again manually moved just to one side of the second feature, and that feature was scanned and recorded. The time required to scan both features in this fashion was 3 to 10 minutes, depending on what scanning speed was used. Three temperature readings were taken during this process.

Next the Powerstat was readjusted so as to change the temperature of the furnace. When the temperature had become constant the scanning process was repeated. In this way intensities were measured at a number of temperatures throughout the working range.

The foregoing gives an idea of the experimental procedure used, but there are many experimental details that had to be considered before the actual intensity measurements were made. These are covered in the following subsections.

Optics

The optics were designed to keep the continuous radiation of the heating-tube walls from reaching the spectrograph; yet they had to allow as much as possible of the light emanating from the vapor inside the tube to enter the spectrograph. Figure 1 is a schematic diagram of the optics finally adopted for this purpose. This diagram is intended to illustrate certain details of the optics, and therefore different parts of the diagram are drawn to different scales.

The heating tube is shown at the left of Fig. 1. The graphite diaphragm A acts in combination with the lens stop C to prevent the black-body radiation of the walls of the hot zone from passing the stop C. The cooler graphite diaphragm B blocks most of the black-body radiation of the hot diaphragm A. The lens at C forms an image of diaphragm A on the lens stop D. The part of the image at D corresponding to the hot diaphragm A is blocked out by the lens stop D, but the part of the image corresponding to the emitting gas is allowed to pass through the hole. S represents the slit of the spectrograph. The cylindrical lens at D makes a tall narrow image of the light beam at S so that a larger percentage of the light passes through the vertical slit S.

Originally the quartz window on the end of the King furnace away from the spectrograph was reflecting some wall light into the optical train. The window was removed and reset at such an angle that light reaching it from the walls was reflected up out of the optical train.

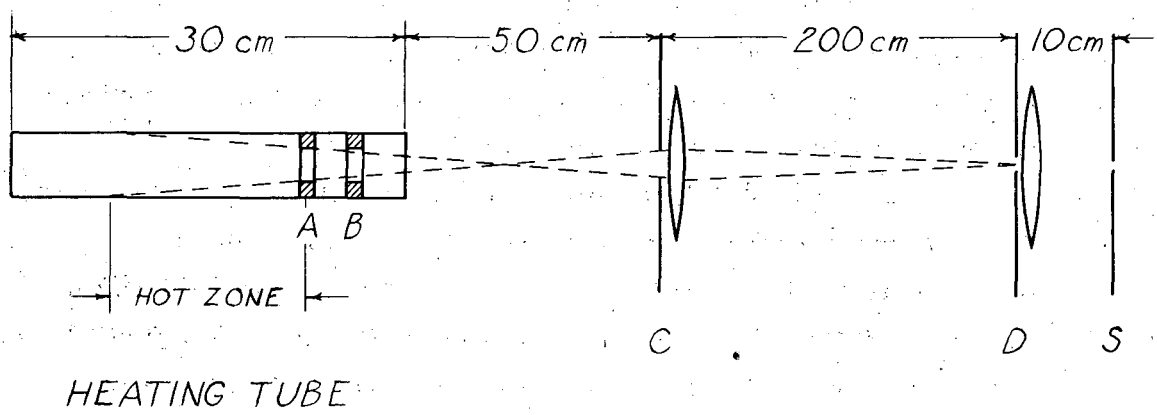

Fig. 1. Schematic diagram of the optics used in the intensity measuring experiments. Different parts of the diagram are drawn to different scales.

Background Radiation

In spite of all these precautions a certain amount of this continuous black-body radiation from the walls of the heating tube still fell on the phototube. This formed a continuous background spectrum over which other spectra were superimposed. It is believed that this remaining background radiation had its origin in particles of solid matter which circulated in the King furnace and which reflected light from the walls of the heating tube into the optics. These solid particles might be caused by disintegration of the vaporizing heating tube and by condensation of carbon and perhaps impurities from the graphite in the cooler parts of the heating tube. The settling of dust particles on parts of the optics outside of the King furnace, and also imperfections in some of the optical parts, may have contributed their share to increasing this background radiation.

As one would predict from the Planck radiation law, this background became more of a problem towards longer wave lengths. Indeed, at the wave length of the Phillips band this background was comparable in intensity to that of the features. Since here the background did not change rapidly with wave length it was easy to distinguish the rotational lines of the Phillips (2-0) band superimposed on the continuum. When intensities were being measured, however, the background did cause some uncertainty because it fluctuated with time and therefore contributed its share to the noise obtained when scanning, especially at large slit widths. These fluctuations in time are probably due to changes in the concentrations of dust particles inside the King furnace.

This background radiation is negligible at the wave lengths of the (0-0) and (1-0) Swan bands; however, in this case their spectra were observed in the second order, and high-intensity first-order background radiation was superimposed on their second-order spectra. Here there was an additional complication in that the apparent intensity of the background radiation as recorded by the Cs_2O cell was rapidly falling off towards longer wave lengths. This was because the

sensitivity of the Cs_2O cell rapidly decreases when one proceeds this far out into the infrared. The superposition of this steeply sloped background on the Swan features made it difficult to measure their intensities. However, this difficulty was easily remedied. A Dow-Corning pyrex filter No. 9788 completely removed the first-order background radiation, while light of the wave lengths of the Swan bands came through almost entirely. It was simply necessary to remember to place the filter in the optical train when one wanted to trace the Swan spectra and remove it when one traced the Phillips spectra. The filter was mounted on a swivel so that the same part of the filter was used every time.

Slit Widths

As we may now see, the selection of slit widths was controlled by several factors. In these measurements the entrance slit of the spectrograph and the slit in front of the phototube were kept at the same width; thus a triangularly shaped line was obtained when scanning. As wide a slit width as possible was used so as to obtain a more intense feature. This increased the signal for a given amount of noise contributed by the photocell at any certain gain; the amount of noise made by the photocell depended only on the gain at which the amplifier was operating and not on how much light was falling on the cell. The second factor was the noise contributed by fluctuations in the background that originated in the furnace. If the slit widths were decreased the intensity of the background would decrease more rapidly than the intensity of the feature. Therefore the ratio of signal to noise of this origin would increase. However, the noise contributed by the background was of a much lower frequency than that of the photocell, and quite often one could trace through a feature without much shift in the background. Therefore a comparatively wide slit of 0.25 mm was used to increase the signal-to-noise ratio of the photocell. This noise level was the main source of error in measuring intensities.

Scanning Speed

The speed used when scanning had an important effect on the intensities measured by this technique. If the phototube scanned past a spectral feature at too high a rate, the recording potentiometer did not have time to make the full response that it would make if the cell remained at rest at the maximum intensity of the feature. This is due to the relatively slow time constant of the electronic circuit. If the percentage of the true peak intensity recorded were less for more intense features than for less intense features, the sigma plot made from the measured intensities would yield a heat lower than the correct value. To find how slowly one had to scan to obtain a heat not suffering from this effect, heats were measured at each of several different scanning speeds. Then a plot was made of the average heat obtained as ordinate versus the scanning speed used when the heat was measured as abscissa. The intercept of this curve with the ordinate corresponds to the true heat.

Measurement of Temperature

Temperature Scale

In order to insure a well-defined temperature scale the No. 2 pyrometer Leeds and Northrup serial No. 749235, which was used for all these measurements, was compared before and after the intensity measurements were made with No. 3 pyrometer, Leeds and Northrup serial No. 709371.* This pyrometer had been standardized by the National Bureau of Standards in Washington, D. C. in January 1956 on the basis of the 1948 thermodynamic temperature scale.[6] The standardized pyrometer was used only for comparison purposes.

---

*Two pyrometers are referred to in this thesis. They belong to the high-temperature section of the University of California Radiation Laboratory. The numerals 1 and 2 appear on the faces of their respective potentiometers.

Its scale correction amounted to minus 88° when the pyrometer read 2800°C and minus 34° when it read 2400°C according to the NBS corrections. When No. 2 pyrometer was compared with this instrument by sighting both instruments on a constant-temperature source, No. 2 read 15° ± 4° higher than No. 3 from 2300°C to 2700°C. When recompared after all the intensity measurements were made, the difference in the readings of pyrometers remained the same within experimental error.

It is believed that Krikorian[19] used the same pyrometer (No. 2) for his measurement as was used in this work; however, at that time there was no recently calibrated pyrometer with which to compare it. Therefore to obtain his temperature scale he calculated the heat for the reaction;

$$ZrC \text{ (solid with excess graphite)} = Zr^{*} \text{(gas in excited state)} + C\text{(graphite)}. \qquad (4)$$

Then he measured this heat by observing the variation of the intensity of the particular electronic transition of zirconium that arises from the excited state as a function of temperature. The heat that he thus obtained agreed with his calculated heat for the reaction of 254.7 kcal at 3000°K. Thus the uncorrected relative temperature readings of the pyrometer were correct within the accuracy with which the heat could be measured, which is about 10 kcal.

Now we shall see that if we correct Krikorian's measured temperatures by amounts determined by the recent Bureau of Standards calibration of pyrometer No. 3 plus the comparison of Nos. 2 and 3 we are led to a serious discrepency between the measured and calculated heat for the above reaction. Since the measured heat was obtained from the slope of a straight-line plot of sigma (which is a function of the intensity of the zirconium feature) versus the reciprocal of the temperature, we may say

$$\Delta H^{\circ}_{3000} = (\Sigma' - \Sigma'')/(1/T'' - 1/T'),$$

where the prime indicates the point at the highest temperature at which Krikorian made his measurements and the double prime indicates the point at the low end of his temperature range. Now if we substitute in this fraction the difference in the reciprocals of the temperatures determined by correcting Krikorian's measured values to the Bureau of Standards temperature scale, we increase the measured heat by more than 11% to 284 kcal. Using a more recent value for the heat of sublimation of zirconium[35] we obtain a slightly higher value than Krikorian calculated for the heat of Reaction (4), namely 258.2 kcal at 3000°K. However, the discrepency between this value and the measured one is too great to be taken into account by the experimental error.

There are two possible explanations why Krikorian's measured heat might be off this far. One is that there was solid solubility between his ZrC and the excess graphite in his heating tube. However, he had samples of his ZrC analyzed by X-ray diffraction before and after his measurements and found no evidence of a change in the lattice constants. Furthermore, if there were solubility between the two solid phases we would expect this to lower his measured heat for Reaction (4) below the value calculated, assuming no solubility. Another possibility is that large temperature gradients developed in his heating tube during the process of the run. However, if he read the temperatures near the high end of the gradient--as is probably the case--the heat measured would again be low.

In view of this discrepency an independent calibration of pyrometer No. 2 was made. This calibration, which was based on the transmissions of the filter screens of the pyrometer, is described in detail in Appendix A. Suffice it to say here that this calibration, using the filter transmissions, showed the National Bureau of Standards calibration of No. 2 to be considerably in error in the temperature range in question. Using the new corrections for No. 2 found in Appendix A to correct Krikorian's measured heat for the Zr reaction, we obtain a value of 260 kcal compared with a value of 258.2 kcal based on the measurements by other observers. Therefore this new temperature scale was used to obtain all the heats presented in this thesis.

Window Correction

In addition to these pyrometer-scale corrections, the temperatures read through the window of the King furnace had to be corrected for reflection losses at the glass-to-air surfaces. For this purpose we may use the Wien's law expression: $1/T_1 - 1/T_2 = K$. If T_2 is the actual temperature of the walls expressed in degrees Kelvin, then T_1 is the absolute temperature that is read through the window. K is a constant that is a function of the transmission of the window. The value of K was determined by reading the brightness temperature of a tungsten filament lamp with the pyrometer, then interposing the window between the pyrometer and the lamp and reading the brightness temperature again. The constant found in this way for the window was $(0.048 \pm 0.003)\ 10^{-4}$ deg.$^{-1}$. The value found by Krikorian for the same window was 0.046×10^{-4} deg.$^{-1}$.

Temperature Gradient

The accuracy with which the intensity variation with temperature could be measured was limited by the temperature gradient of the heating zone of the tube. Although these tubes were quite uniform in temperature to start with, during the process of a run hot spots began to appear in the walls of the tube. These hot spots were self-inductive for two reasons. The higher temperature of the area caused this part of the tube to vaporize and to be attacked by residual oxygen more rapidly than the cooler parts of the tube. Thus the heating tube became thinner at this point; the resistance rose, and consequently more power was dissipated at this point. In addition, vaporizing metallic impurities condensed on the first cool surface with which they came in contact. The result was that a shiny reflecting coating was deposited on the first radiation shield opposite the hot spot. This in turn increased the effectiveness of the radiation shield, causing an even greater temperature gradient.

Several steps were taken to minimize this gradient production. The first was to experiment with the dimensions and wall thicknesses of the heating tube until a design was found that produced a minimum

initial temperature gradient. The dimensions of the final design adopted were those given in the "Experimental Equipment" section of this paper. Another step was that described by Krikorian, and consisted of inserting a graphite sleeve into the graphite spool that constituted the first radiation shield. When this sleeve became shiny from its coating, it could be discarded and another inserted in its place. During the final measurements, to insure that the minimum of temperature gradient was produced in each run, the heating tube and sleeve were both replaced at the beginning of each run. With this procedure, the temperature gradients amounted to 0 to 30°C at the beginning of each run and varied from 40 to 100°C at the end of a run. The gradients were produced most rapidly at the highest temperatures, and just how large the final gradient became depended on the maximum temperature to which the tube was taken and how long it was held there.

Because of these temperature gradients (sometimes as high as 70 to 80°C), there was ambiguity as to just where in the heating tube the optical pyrometer should be sighted. In order to maintain reproducibility between runs the procedure adopted in these measurements was to aim the pyrometer at the hottest part of the wall that could be observed. As may be seen, this procedure tends to give a heat which is lower than the correct value, if one starts the runs at the lowest temperature and works systematically up to the highest temperature. At the end of the run, when the tube is hottest, the highest gradients are produced in the tube. At this time the intensities observed are produced by a large proportion of molecules at temperatures lower than that read by the pyrometer at the hottest spot on the wall. Therefore the intensity observed at the highest temperature is considerably lower than that which would be observed if all the gas were at the same temperature. This is also true at the lowest temperature but to a considerably smaller extent. This manner of reading temperatures thus tends to give a heat lower than the correct one.

To evaluate the magnitude of this lowering of the heat and to correct for it, the following procedure was used in place of tracing the spectra from the lowest to the highest temperature in chronological

order. The intensities were first recorded at the middle, then at the lowest, than at the highest, and finally again at the middle of the temperature range. Thus in a plot of logarithm of intensity versus the reciprocal of the temperature, the distance by which the last point measured falls below the curve drawn through the other points at the same temperature gives a measure of this gradient effect. Accordingly one may use this deviation in deciding how to weight the various points in the plots of sigma versus 1/T.

If one were to read the temperature of the coolest spot of the heating tube, for analogous reasons one would obtain a heat that is higher than the correct value. However, the hottest spot of the tube could usually be read with greater consistency. For even greater consistency in reading temperatures one might sight the pyrometer on a small graphite plug placed inside the heater tube. This would insure that the pyrometer operator always read the temperature at exactly the same point, and thus eliminate errors arising from not sighting on quite the same part of the tube wall each time. However, this method was not used in the work described here, for the following reason. When even a small-sized plug was introduced into the system, the limiting diaphragms placed in the optical system were not adequate to prevent a great deal of the black-body radiation from the plug from reaching the spectrograph. This continuous radiation had the effect of greatly lowering the sensitivity of the detection system at the wavelength of the Phillips band.

Variation of Temperature with Time

Owing to the development of hot spots in the heating tube and to difficulties in controlling the temperature of the furnace, there occasionally were fluctuations in the temperature of the heating tube in the time that it took to trace through the two features with the phototube. To compensate for this, three temperature readings were taken for each tracing of the two features. The first was taken before the first feature was traced, the second between features, and the third after the second feature had been traced. Generally all three readings

agreed within the experimental accuracy of the pyrometer and showed a random fluctuation with time. In this case the average of the three readings was used for the temperature of both features in the sigma plots. Occasionally, however, the discrepancy in the readings fell outside this experimental error, and the readings showed a systematic variation with time. In this case the average of the first and second readings was taken as the temperature of the first feature; the average of the second and third readings was used for the temperature of the second feature traced.

Rotational Temperatures

As a check on these procedures for measuring temperatures, an attempt was made to determine the gas temperatures by using the relative intensities of the rotational lines of the Phillips (2-0) band. It turned out, though, that this means of determining the gas temperature was too insensitive for this purpose, because the rotational states are too close in energy. The temperatures thus determined from a single tracing using different sets of rotational lines varied by 200° or 300°C; they agreed within this variation with the wall temperature of the heating tube as observed by the optical pyrometer.

CALCULATION OF RESULTS

Heats from Sigma Plots

We may use the second law of thermodynamics to calculate heats of formation of the singlet and triplet states of C_2 from intensity measurements of transitions that arise from these states. Consider the reaction

$$2\ C\ (\text{graphite}) = C_2'\ (\text{gas in a particular rotational, vibrational and electronic state}) \qquad (5)$$

For this reaction we may write the van't Hoff equation,

$$\frac{d(\ell n\ P'_{C_2})}{d(1/T)} = -\frac{\Delta H_T^{o_1}}{R} \qquad (6)$$

Here P'_{C_2} is the equilibrium pressure of C_2 gas in the particular rotational, vibrational, and electronic state designated in Eq. (5), $\Delta H_T^{o_1}$ is the heat of Reaction (5), and R is the universal gas constant.

At low concentrations the intensity of an emission feature is directly proportional to the concentration of the excited state giving rise to the transition. At higher concentrations this relationship no longer holds, owing to the phenomenon of self-absorption. Self-absorption is present in a column of gas because the molecules that are closer to the observer tend to absorb part of the ratiation emitted by the molecules further away in the column. This effect was found to be present in both the Phillips (2-0) band and the Swan (0-0) and (1-0) bands in the temperature range over which the measurements were made; therefore the magnitude of this effect had to be known before heats could be accurately calculated.

A means of experimentally evaluating this self-absorption effect is developed in Appendix B for a monochromatic measurement. In this section a correction factor is found which, when multiplied with the intensity measured at a single wavelength, yields a quantity directly proportional to the concentration of the molecule in its excited

state. In Appendix C this monochromatic correction factor is integrated over the Doppler profile of the Phillips rotational line. Thus a correction factor is developed which is applicable to the measured integrated intensity of this feature. The final correction factors used for the Phillips rotational line are presented in Table VI in Appendix C as a function of the temperature. In Appendix D the correction factors for the measured intensity of the Swan-band heads are developed and tabulated as a function of temperature.

Let us call this correction factor Q'. The corrected intensity $Q'I'$ is directly proportional to the concentration of molecules in the excited state. Thus by applying the ideal gas law we may solve for the pressure in terms of the corrected intensity:

$$kQ'I' = N'/V = P'_{C_2}/RT.$$

In this equation, $\underline{k}$ is a constant and $\underline{N'}$ is the concentration of C_2 gas in the particular excited state. Then we have

$$P'_{C_2} = k\,RQ'I'T. \qquad (7)$$

Also for Reaction (5) we may write

$$\Delta H^{o\prime}_T = \Delta H^{o\prime}_{3000} - \Delta C^{o\prime}_p (T - 3000), \qquad (8)$$

where $\Delta C^{o\prime}_p$ is the change in heat capacities for Reaction (5). The $C^{o\prime}_p$ for C_2 gas in a single rotational state is simply 5/2 R at any temperature, since its only degrees of freedom are those of translation. The heat capacity of graphite has been measured at 3000°K by Rasor, who gives a value of 6.2 eu.[30] The value for this quantity given by the National Bureau of Standards, 6.42 eu, is within his experimental error.[32] Since we later on use the NBS value for the heat content of graphite at 3000°K, we shall use their value here for consistency. One then obtains a $\Delta C^{o\prime}_{p3000}$ for Reaction (5) of -7.87 eu, which we shall assume is constant with temperature over the narrow range in which we use it.

Now if we substitute Eqs. (7) and (8) with the value of ΔC_p^o just calculated into Eq. (6) and integrate, we obtain

$$\Sigma' = R\ell n\,(Q'I'T) + 7.87\,\ell n\,T + 7.87\,3000/T = -\Delta H^{o\,\prime}_{3000}/T + K'. \quad (9)$$

Let us consider that the single prime applies to C_2 gas in a particular rotational level of the $v' = 1$ or 0 vibrational level of the $^3\Pi_g$ state. This is the upper electronic state of the Swan bands. We may then write an equation similar to (9), replacing the single primes with double primes. The double primes signify quantities related to a particular rotational level of the $v' = 2$, $^1\Pi_u$ state of the Phillips bands. Since in this case ΔC_p^o is also -7.87 eu, the equation is

$$\Sigma'' = R\,\ell n\,(Q''I''T) + 7.87\,\ell n\,T + 7.87\,3000/T = -\Delta H^{o\,\prime\prime}_{3000}/T + K. \quad (10)$$

Now we may subtract Eq. (10) from Eq. (9) and obtain

$$\Sigma = \Sigma' - \Sigma'' = R\ell n\,(Q'I'/Q''I'') = (\Delta H^{o\,\prime\prime}_{3000} - \Delta H^{o\,\prime}_{3000})/T + K = -\Delta E/T + K. \quad (11)$$

ΔE is the energy difference between the emitting levels of the upper states of the Swan transition and the Phillips transition. Thus if we plot Σ', Σ'', or Σ versus $1/T$, using the intensity versus temperature measurements, we should obtain a straight line whose slope is the negative of the heat of formation of a level of the $^3\Pi_g$ or the $^1\Pi_u$ state of C_2 gas from solid graphite, or the difference in energy between these levels, respectively.

To evaluate the slope of the three sigma equations given above, a number of runs were made at several different scanning speeds; in each run the two spectra were scanned at from ten to fourteen different temperatures each with a fresh heating tube. As the measurements progressed a number of improvements were made in the sensitivity of the equipment; they extended the lower end of the temperature range, where significant intensities could be measured, by 200°. This in turn improved the accuracy of the heats by yielding a greater range over which the intensities could be measured and by allowing one to measure the intensities at temperatures where self-absorption corrections were of a much smaller magnitude.

The data from a typical run made with this improved sensitivity are presented in Table I. The temperature scale is the one adopted in Appendix A; Σ', Σ'', and Σ are calculated from the intensities and temperatures by Eqs. (9), (10) and (11). The scanning speed used in this run was approximately 21A per minute in the first order and 10.5 A per minute in the second order; the slit widths were 0.20 mm. In Figs. 2, 3, 4 are presented the plots of Σ', Σ'', and Σ, respectively, versus $1/T$. The points in these graphs are numbered to show the chronological order in which they were measured. The solid line is the best straight line that could be drawn through the points by eye. In drawing this line allowance was made for the development of a temperature gradient at the maximum temperature reached. The affect of the gradient was evidenced by the distance by which point No. 14, measured after the tube had been at maximum temperature, fell below the points taken previously at the same temperature. A least-squares method of drawing a straight line was not used because this method would place too much emphasis on the inaccurate end points of the plots if no weighting were used. The values obtained from these plots for $\Delta H^{o\prime}_{3000}$, $\Delta H^{o\prime\prime}_{3000}$, and ΔE were 235, 221, and 20.2 kcal per mole, respectively.

Uncertainty in Measured Heats

There are three possible sources of uncertainty in these figures. The first is the self-absorption corrections, the second is measurement of intensities, and the third is the measurement of the temperature of the column of gas. The error introduced by inaccuracies in the heat-capacity data is negligible, as a large change in ΔC_p^o has little effect on the slopes of Figs. 2 or 3 and does not change the slope of Fig. 4 at all. It may easily be shown that the uncertainty introduced by the self-absorption corrections is also negligible, for the corrections contribute only 2.36, 0.483, and 1.88 kcal to the values of $\Delta H^{o\prime}_{3000}$, $\Delta H^{o\prime\prime}_{3000}$, and ΔE. The uncertainty in these contributions could not amount to more than a few percent.

Table I

Intensities measured at different temperatures in a typical run. Σ', Σ'', and Σ are calculated from these data by Eqs. (9) (10) and (11), respectively. Primes refer to Swan transition and double primes to Phillips transition.

Sequence	T (°K)	I' measured	Q'I' corrected	Σ' (eu)	I'' measured	Q''I'' corrected	Σ'' (eu)	Σ (eu)	$1/T \cdot 10^4$ ($^\circ K^{-1}$)
5	2666	1.4	1.4	87.29	1.8	1.8	87.79	-0.500	3.751
4	2714	4.7	4.7	89.72	4.1	4.1	89.45	+0.271	3.685
6	2718	4.8	4.8	89.76	6.4	6.4	90.33	-0.572	3.679
3	2784	11.0	11.0	91.39	10.3	10.3	91.26	+0.130	3.592
7	2791	15.1	15.1	92.07	14.8	14.8	92.03	+0.040	3.583
2	2838	25.8	26.0	93.18	24.5	24.5	93.06	+0.118	3.524
8	2855	39.9	40.2	94.05	43.2	43.2	94.20	-0.143	3.503
1	2877	51.2	51.7	94.56	41.8	41.9	94.15	+0.417	3.476
9	2926	102.1	103.9	95.98	104.2	104.4	95.99	-0.010	3.418
10	2954	140.2	143.7	96.59	119.9	120.4	96.29	+0.303	3.385
14	2966	128.1	131.8	96.42	110.5	111.1	96.14	+0.283	3.372
11	2988	210.8	218.2	97.43	164.7	165.7	96.95	+0.479	3.347
12	3012	243.0	254.2	97.72	214.6	216.3	97.49	+0.231	3.320
13	3037	361.7	383.4	98.53	289.7	292.9	98.11	+0.420	3.293

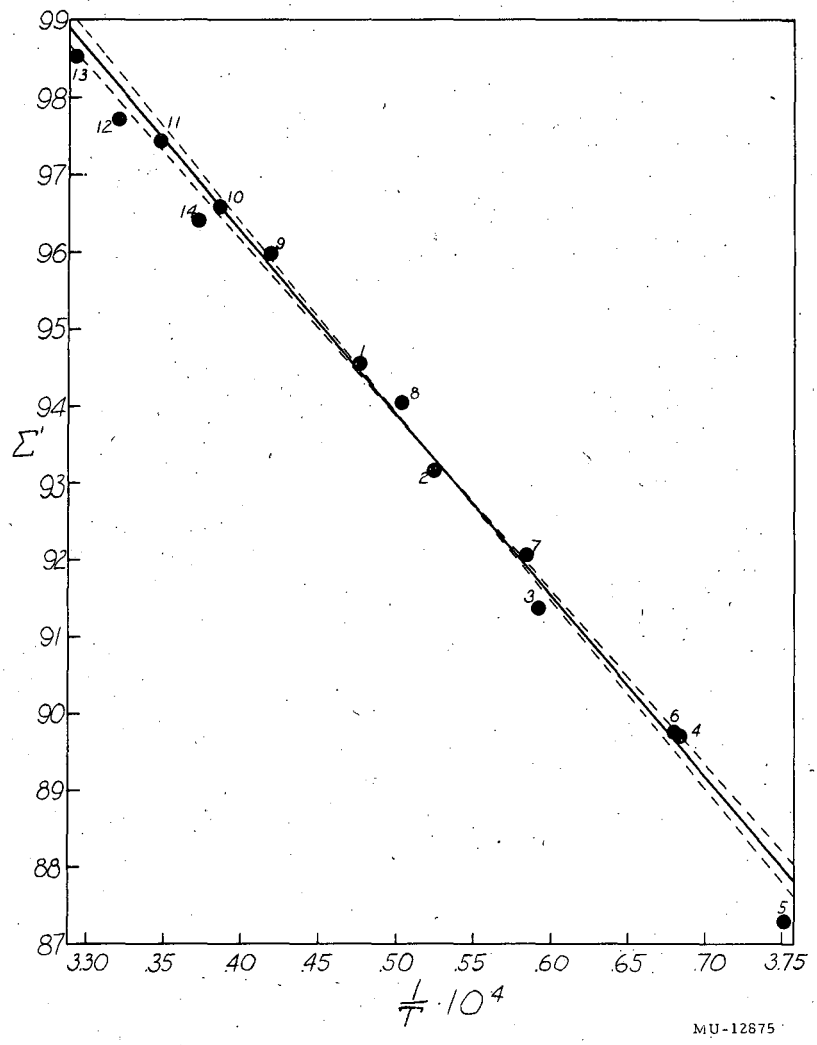

Fig. 2. Σ'-versus-1/T plot from the data of Table I. The points are numbered in the order in which they were measured. The solid line is the best straight line that could be drawn through the points by eye. The dashed lines show the limits of uncertainty in the slope of the line.

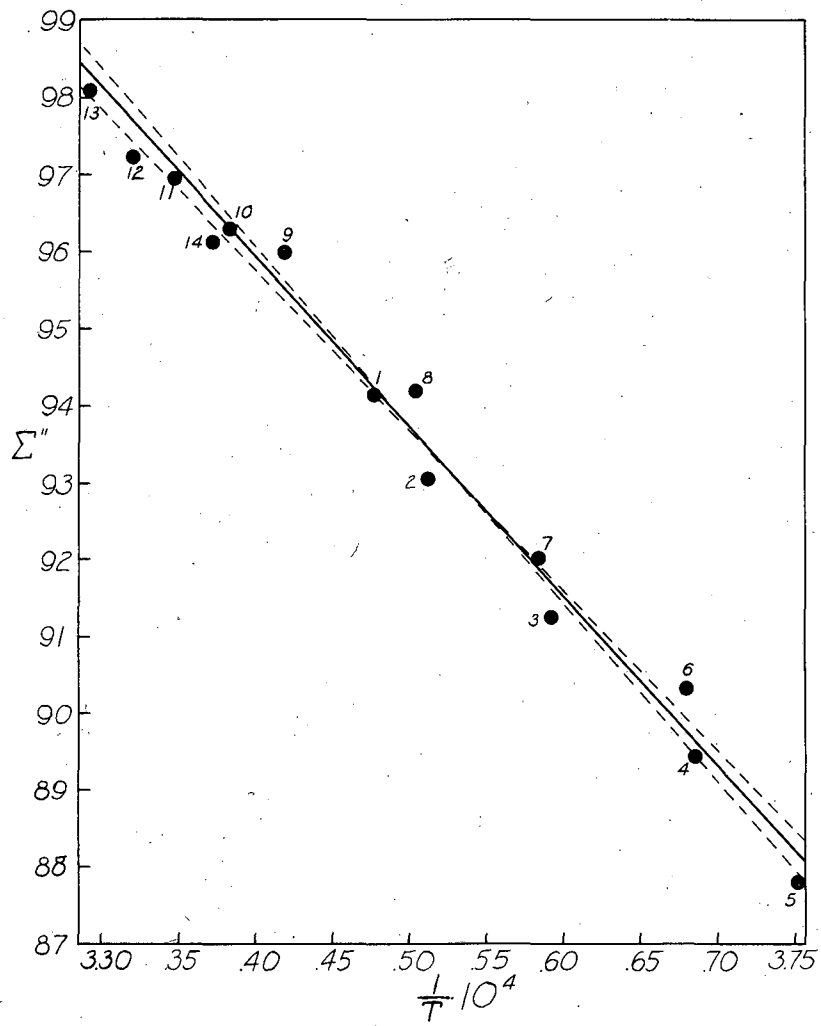

Fig. 3. Σ''-versus-1/T plot from the data of Table I. The points are numbered in the order in which they were measured. The solid line is the best straight line that could be drawn through the points by eye. The dashed lines show the limits of uncertainty in the slope of the line.

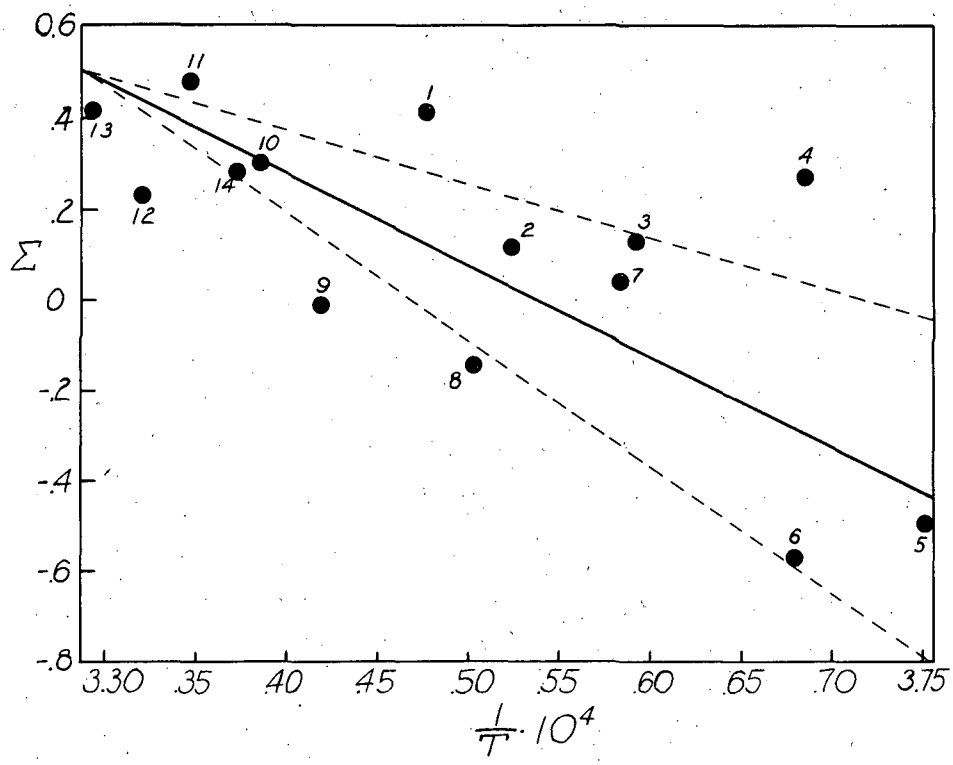

Fig. 4. Σ-versus-1/T plot from the data of Table I. The points are numbered in the order in which they were measured. The solid line is the best straight line that could be drawn through the points by eye. The dashed lines show the limits of uncertainty in the slope of the line.

The uncertainty of the intensity measurements may be evaluated quite accurately. The accuracy of the intensity measurements is limited by the noise level present in the instrument when the features are being traced. This noise level may be ascertained by examining the recording of the background intensity traced just before and after the feature was recorded. For the Swan bands the total fluctuation in intensity amounted to 1.2 intensity units quoted on the same scale as that used for intensities in Table I. This noise level did not depend on the intensity of light falling on the photocell, and was proportional to the particular gain of amplification used. This seems to indicate that the source of this noise was a fluctuation in the dark current of the cooled photocell itself. This total fluctuation of the intensity of 1.2 units produced an uncertainty in the measured intensity of the feature of ± 0.6 unit, since only the peak of the feature is subject to this uncertainty; the fluctuations in the background could be averaged out by drawing the best straight line through the traced curve.

The uncertainty in Σ' for any point of Fig. 2 due to this fluctuation in intensity may be obtained by differentiating Eq. (9) with respect to $Q'I'$, thus obtaining $d\Sigma' = R/Q'I'\, d(Q'I')$, where $d(Q'I')$ is simply 0.6 unit. In this way we find the uncertainty in Σ' to be 0.9, 0.4, 0.03, and 0.003 eu for points Nos. 5, 6, 8, and 13, respectively. Deviations of points in Fig. 2 by amounts greater than these are due to uncertainties in measuring the temperature. The uncertainty in the heat determined from Fig. 2 due to intensity measurement may be calculated by considering this quantity to be equivalent to the uncertainty in the heat determined from a two-point plot. One point of this plot would be the point No. 13, which has negligible uncertainty, and the other would be point No. 8, which is the median point in the actual plot in intensity and uncertainty. The uncertainty of the two-point plot may be obtained from the above calculated values of $d\Sigma'$ and the formula $\Delta H^{o\prime}_{3000} = \Delta\Sigma'/\Delta(1/T)$.* Thus we obtain

*This uncertainty might be calculated more accurately by averaging the uncertainties of each set of two points, taking point No. 13 as one point and each other point in the plot as the other point. However, the above approximation presumably gives close enough results for this purpose.

an uncertainty in the heat calculated from Fig. 2 due to intensity measurement of 1.6 kcal per mole.

In the Phillips rotational line the total fluctuation in the intensity of the background was equal to 3.3 units. This fluctuation is considerably greater than for the Swan bands, since at this wavelength the background intensity arising from dust clouds in the King furnace, which vary in concentration with time, is many times its size at the wavelength of the Swan bands. Here again, though, the noise is proportional to the gain of amplification being used. The uncertainties in Σ'' calculated by the same method as above for points Nos. 5, 6, 8, and 13 amount to 2, 0.6, 0.1, and 0.13 eu. Using the same methods as above, we obtain an uncertainty due to intensity measurement of 5.8 kcal per mole for the heat calculated from the plot of Fig. III.

The uncertainty in Σ for each of the points of Fig. 4 may be calculated by taking the square root of the sum of the squares of the uncertainties of the points in Figs. 2 and 3, since Σ is simply the difference between Σ' and Σ'' for each point. Thus the uncertainties in the individual points Nos. 5, 6, 8, and 13 in Fig. 4 are 2, 0.8, 0.1, and 0.013 ue, respectively. Furthermore the uncertainty in the heat obtained from the slope of Fig. 4 may be calculated by taking the square root of the sum of the squares of the uncertainties due to intensity measurement in the heats of Figs. 2 and 3. Thus the ΔE quoted is uncertain by 6.0 kcal per mole due to the measurement of intensities.

The other source of uncertainty in the heats lies in the measurement of the temperature of the column of gas. If we assume that the final temperature scale adopted was correct, then the main source of error in this respect is the development of a temperature gradient in the heating tube during the process of a run. If the average gradient of the heating tubes was 10° at the beginning of a run and 60° at the end of a run, then the uncertainty of the individual points might be considered to be as high as 50° at the high-temperature part of the run with respect to the points at the beginning of the run; the high end of the gradient was the temperature recorded all through the run. However, since the intensities of the spectra depend exponentially on the temperature, the

effective temperature of an emitting gas in such a gradient would be above the middle temperature of the gradient; thus the uncertainty in the individual points is only 25° at the end of the run. Furthermore, since the straight line was drawn so as to cancel out the effects of this temperature gradient, we might expect the uncertainty in the slope of this line to amount to only about 12° in the range of 400° over which the measurements were made.

Another source of error in measuring the temperature occurs;--sometimes the temperature of the heating tube drifted between the time when the Phillips rotational line was traced and when the Swan band was traced. This variation amounted to about 10° if a moderately fast scanning speed (10.5 A per minute) was used. Since for such a fluctuation an average of the two extreme readings was used in calculating the points of Figs. 2 and 3, we might expect this source to produce an uncertainty of 5° in the points of these plots. However, a variation in the furnace temperature between the times of scanning the two features may cause the resulting point to deviate from constant temperature points by an amount equivalent to 100°. This is because the ratio of the intensity of the Swan band to the Phillips line measured at a constant temperature changes much more slowly with temperature than either intensity by itself changes with temperature. Thus let us say that the total uncertainty in temperature amounts to 17° in 400° in Figs. 2 and 3, or 4% of $\Delta(1/T)$, and about 112° in the 400° range of Fig. 4, which is 28% of $\Delta(1/T)$. Thus the uncertainty in ΔH^{o}_{3000} and ΔH^{o}_{3000} due to inaccuracies in the measurement of temperature amounts to 9 kcal per mole, and in ΔE to 5.7 kcal per mole.

We may obtain the total uncertainties in ΔH^{o}_{3000}, ΔH^{o}_{3000}, and ΔE by taking the square root of the sum of the squares of the uncertainties in these figures due to intensity and temperature measurement. Thus we obtain total uncertainties of 9, 11, and 8.3 kcal per mole, respectively. These uncertainties are indicated in Figs. 2, 3, and 4 by the dotted lines.

We now see that variations in temperature between the tracings of the two features prevented us from realizing the full accuracy predicted in the introduction of this thesis for determining ΔE by measuring the ratios of the intensities of the two features. Nevertheless, by tracing both features simultaneously, we obtain an uncertainty of 8.3 kcal per mole as opposed to an uncertainty of 14 kcal per mole that would be realized if the two heats were determined separately and subtracted.

The Heat of Formation and Ground State of C_2 Gas

One may calculate ΔH_0^o, the enthalpy change at 0^oK, for the reaction

$$2C \text{ (graphite)} = C_2 \text{ (gas)} \qquad (2)$$

by correcting to 0^oK the heat of formation at 3000^oK of either the $^3\Pi_g$, $v' = 0$ or 1, $J' = 17$* state or the $^1\Pi_u$, $v' = 2$, $J' = 32$ state and subtracting its excitation energy above the lowest rotational level of the lowest vibrational state of the $^3\Pi_u$ or $^1\Sigma_g^+$ state, depending on whether the $^3\Pi_u$ or the $^1\Sigma_g^+$ state is the ground state of C_2. At 0^oK all the molecules of C_2 gas will be in the lowest rotational level of the lowest vibrational state of its ground state.

We may correct $\Delta H^{o\prime}_{3000}$ to 0^oK by taking account of the heat contents at 3000^oK of both sides of Reaction (5). For the single excited state of C_2 we obtain for $(H^{o\prime}_{3000} - H^{o\prime}_0)$ simply (5/2) R 3000. For graphite the National Bureau of Standards gives a value of 15.03 kcal for $(H^o_{3000} - H^o_0)$.[32] It then follows that $(\Delta H^{o\prime}_{3000} - \Delta H^{o\prime}_0)$ for Reaction (5)

*The $J' = 17$ level is used in the following calculations because the rotational line in the P branch arising from this level is the central line contributing to the head of the (0-0) and (1-0) bands as recorded by the instrument. It is felt that attributing the temperature coefficient of the intensity of this head to this centrally located line is justified, since the relative intensities of the rotational lines contributing to the head change only slightly over the narrow temperature range used in this experiment.

is equal to -15.16 kcal per mole. We may also calculate the excitation energy of the J' = 17, v' = 0 level of the $^3\Pi_g$ state above the lowest level of the $^3\Pi_u$ state. The rotational energy of this level is 533.88 cm^{-1}; the vibrational and electronic contribution is 19,378.50 cm^{-1}. Thus its total excitation amounts to 19,912.38 cm^{-1} or 56.92 kcal. Thus if $^3\Pi_u$ is the ground state of C_2, we may say that the heat of Reaction (2) at 0°K is $\Delta H_0^o = \Delta H_{3000}^{o'} - 41.76$ kcal per mole, where $\Delta H_{3000}^{o'}$ is the slope of the straight line obtained by plotting Σ' of Eq. (9) against 1/T, using the intensities measured for the (0-0) Swan band head. If instead we measure the Swan (1-0) head, we obtain the following excitation energy: rotational contribution, 528.95 cm^{-1}, plus vibrational and electronic contribution, 21,133.84 cm^{-1}, equals total excitation, 21,662.79 cm^{-1} or 61.92 kcal per mole. Thus when one uses the Swan (1-0) band head the result is $\Delta H_0^o = \Delta H_{3000}^{o} - 46.76$ kcal per mole.

In the same way, if we assume for the moment that $^1\Sigma_g^+$ is the ground state of C_2, we may calculate ΔH_0^o for Reaction (2) from $\Delta H_{3000}^{o''}$. The excitation energy of the J' = 32, v' = 2 level of the $^1\Pi_u$ state above the lowest level of the $^1\Sigma_g^+$ is as follows: rotational energy, 1654.76 cm^{-1}, plus vibrational and electronic contribution, 11,412.31 cm^{-1}, equals total excitation energy, 13,067.06 cm^{-1} or 37.35 kcal per mole. Thus if $^1\Sigma_g^+$ is the ground state of C_2, since $(\Delta H_{3000}^{o''} - \Delta H_0^{o''})$ is also -15.16 kcal per mole, we have $\Delta H_{3000}^{o''} = 22.19$ kcal per mole.

From the difference in energy of the upper levels of the two transitions as obtained from the Σ plot of Eq. (11) we may calculate the difference in energy of the lowest levels of the $^3\Pi_u$ and $^1\Sigma_g^+$ states since we know the excitation energies of the upper states. Thus the difference in energy between the lowest levels of the $^3\Pi_u$ and $^1\Sigma_g^+$ states is $\Delta E_0 = \Delta E - 19.57$ or 24.57 kcal depending on whether one is comparing the Swan (0-0) or (1-0) band head with the Phillips (2-0) rotational line. The quantity ΔE_0 is so chosen that it will turn out positive if the $^1\Sigma_g^+$ state is the lowest, negative if the $^3\Pi_u$ state is the lowest state.

A total of seventeen intensity-measuring runs were made at three different scanning speeds to determine $\Delta H^{o\prime}_{3000}$, $\Delta H^{o\prime\prime}_{3000}$, and ΔE. From the data of these runs Σ', Σ'', and Σ plots were made as illustrated for a typical run in the last section. From the $\Delta H^{o\prime}_{3000}$, $\Delta H^{o\prime\prime}_{3000}$, and ΔE values obtained from the slopes of these plots $\Delta H^{o\prime}_0$, $\Delta H^{o\prime\prime}_0$ and ΔE_0 were calculated; the corrections shown in the preceding paragraphs were used. In Table II are tabulated the averages of these three heats obtained in a set of runs at each of the three scanning speeds. Presented next to each of these heats is the average deviation of an individual run in that set of runs. The set of runs at the highest scanning speed was made with the Swan (0-0) band and slits varying from 0.10 to 0.20 mm, constant for each run. The runs at other speeds were all made with the Swan (1-0) band and slit widths of 0.20 mm.

Table II

Heats of formation at 0°K of the $^3\Pi_u$ and the $^1\Sigma_g^+$ states of C_2 and the difference in energy between them as determined at three different scanning speeds. Av. dev. stands for the average deviation of the individual values in each set of heats.

Speed* (A/min)	No. of runs	$^3\Delta H^{o\prime}_0$ ($^3\Pi_u$ state, kcal/mole)	Av. dev.	$^1\Delta H^{o\prime\prime}_0$ ($^1\Sigma_g^+$ state, kcal/mole)	Av. dev.	ΔE_0	Av. dev.
84.0	4	184	9	162	5	+26.3	5.2
21.0	9	192	8	196	9	- 2.8	7.1
5.25	4	204	6	212	10	- 5.0	11.1

As was predicted, Table II shows the heats of formation of the two states increasing significantly as the speed of scanning in the intensity measurements which led to these values was decreased. Since the width of the Phillips rotational line is considerably narrower than that of the Swan-band head, the effect of scanning rate is much more pronounced in $\Delta H^{o\prime\prime}_0$, the heat of formations of the lower state of the Phillips transition than in $\Delta H^{o\prime}_0$, the heat of formation of the lower Swan state.

*The scanning speeds quoted in the table are when scanning the first-order spectrum. The corresponding speeds for the second order are 42.0, 10.5, and 2.63 A per minute, respectively.

This has a considerable effect on ΔE_0, the difference in energy between these two states, since the apparent height of the $^1\Sigma_g^+$ state increases more rapidly than that of the $^3\Pi_u$ state with decreasing scanning speed.

It will be noted that the average deviation of the individual run in each set of runs came out to be the same as or less than the uncertainties predicted for the different values of the heats in the preceding section. An exception is ΔE_0 at the lowest scanning speed. This is not surprising, as the slower the scanning speed the greater is the chance that the temperature of the furnace will change during the time interval between the scanning of the two features. Thus the average deviation at this scanning speed lies outside of that expected for a more rapid scanning rate. The uncertainty in the average heat from a set of runs may be expressed as the uncertainty of an individual run divided by the square root of the number of runs in the set.

To obtain the best values for $\Delta H_0^{o_I}$, $\Delta H_0^{o_{II}}$, and ΔE_0, plots were made of the apparent values of these quantities against the scanning rates at which they were measured; the correct value for these heats is the interception of these curves with the zero scanning-speed ordinate. These plots are shown in Figs. 5, 6, and 7. In these plots the height of each point shows the uncertainty calculated for the average heat of that particular set of values.

There is some uncertainty involved in extrapolating the curves of Figs. 5, 6, 7 to zero scanning speed in that no point has been determined below a scanning rate of 5.25 A per minute. This uncertainty would not have been relieved by measuring a point at a still lower scanning rate; such a point would have a much greater uncertainty than those shown, owing to the greater length of time required to scan the two features.

In order to extrapolate the curves of Figs. 5, 6, 7 to the ordinate the properties of the limiting slope of the curves had to be determined. In Appendix E the nature of the limiting slope is derived on the basis of the properties of the detecting and recording equipment. The result of these calculations indicates that the curves of Figs. 5, 6, 7 should be extrapolated to the ordinate by drawing straight lines tangent to the curves at the points measured at the lowest scanning speed.

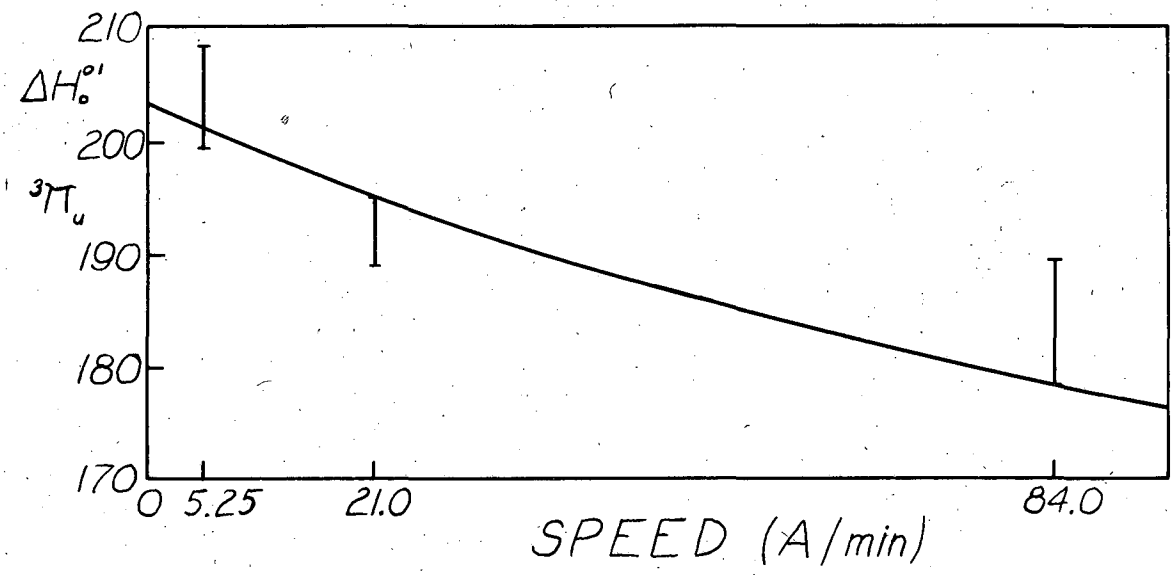

Fig. 5. Heat of formation at 0°K of the $^3\Pi_u$ state of C_2 determined at three different scanning speeds. The heights of the points represent the uncertainties in the heats. The correct heat corresponds to the intersection of this curve with the ordinate.

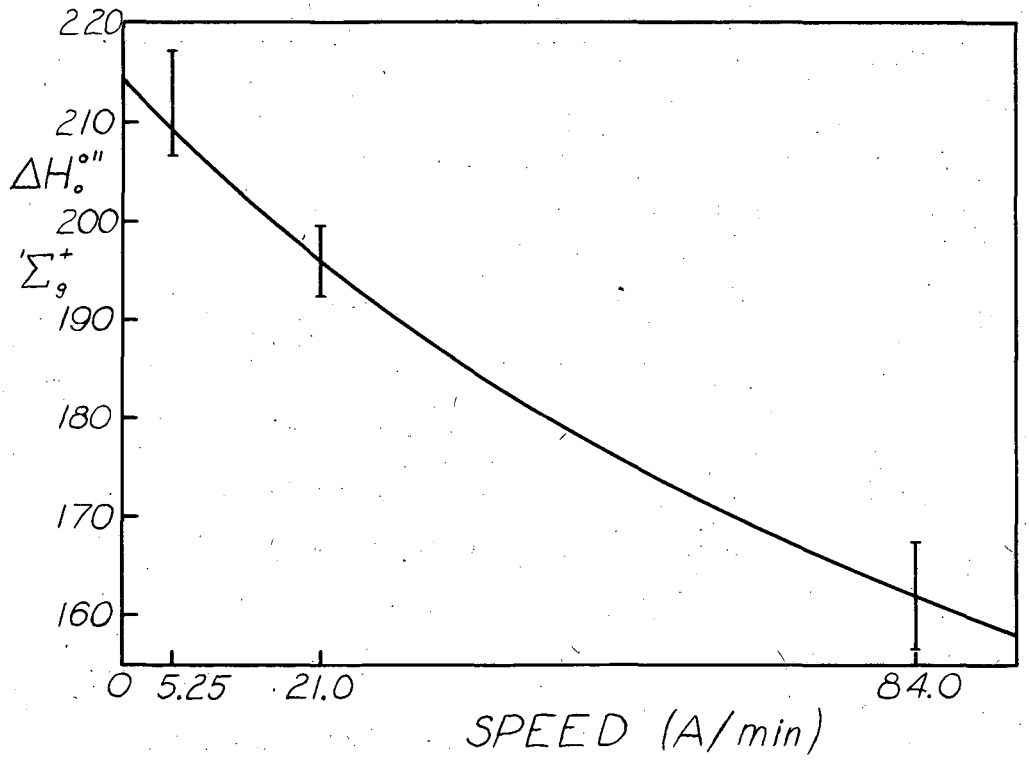

Fig. 6. Heat of formation at $0^{\circ}K$ of the $^1\Sigma_g^+$ state of C_2 determined at three different scanning speeds. The heights of the points represent the uncertainties in the heats. The correct heat corresponds to the interception of this curve with the ordinate.

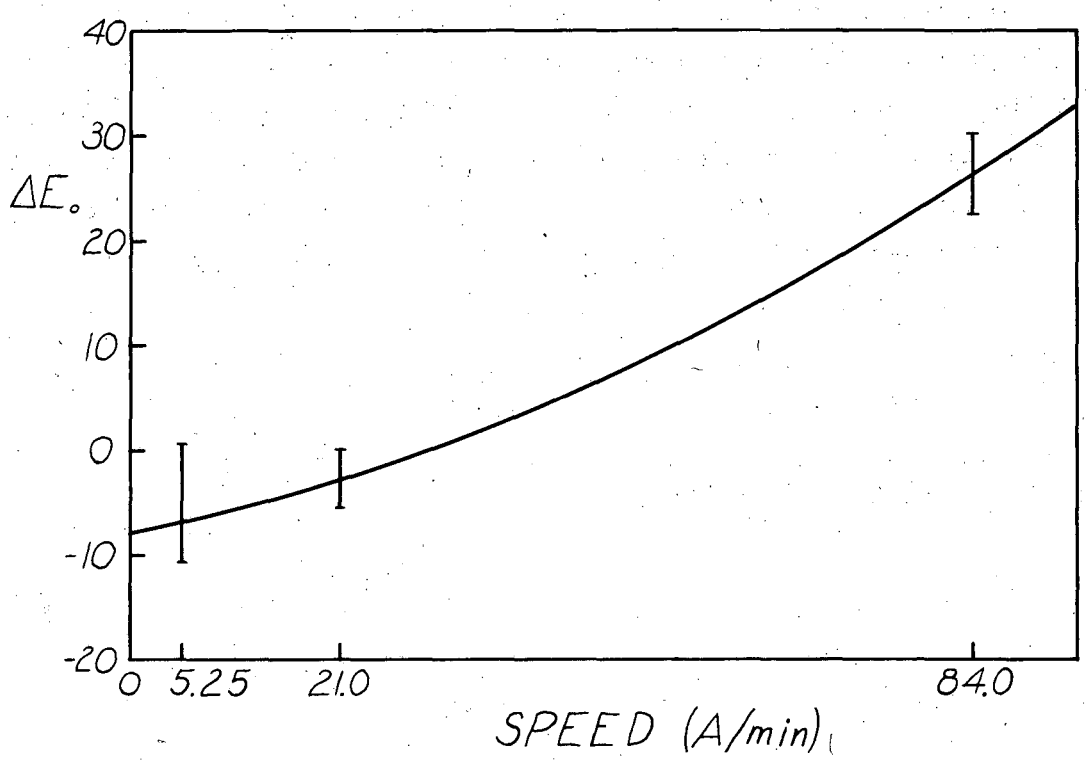

Fig. 7. Difference in energy between the $^3\Pi_u$ and the $^1\Sigma_g^+$ states of C_2 determined at three different scanning speeds. The heights of the points represent the uncertainties in the heats. The correct energy difference corresponds to the interception of this curve with the ordinate. A negative value for this quantity means that the $^3\Pi_u$ state is lower than the $^1\Sigma_g^+$ state.

This extrapolating procedure gave the following heats: $\Delta H_0^{o_I}$, the heat of formation of the $^3\Pi_u$ state, equals 203 ± 4 kcal per mole; $\Delta H_0^{o_{II}}$, the heat of formation of the $^1\Sigma_g^+$ state, has a value of 214 ± 5 kcal per mole; ΔE_0, the difference in energy between these states, equals -8 ± 4 kcal per mole. The uncertainties given are the averages of the uncertainties of the two points closest to the ordinate in Figs. 5, 6, 7. This result indicates that the $^3\Pi_u$ state is the lowest of the observed states, and probably is the ground state of C_2. The difference in heats determined from Figs. 5 and 6 agrees with the energy value obtained from Fig. 7 within experimental error, but of course the result from Fig. 7 should be regarded as the most accurate value for the energy difference. If we assume that no unobserved state is lower than the $^3\Pi_u$ state of C_2, we may take 203 ± 4 kcal per mole as the best value determined in this work for the heat of sublimation of C_2.

DISCUSSION OF RESULTS

Absorption Experiment

In the introduction of this thesis it was stated that the relative precision of an emission or absorption experiment would be determined by whether the two lower or the two upper states of the Swan and Phillips transitions are closer together. This statement was based on the assumption that the error in determining the energy difference was proportional to the magnitude of the heat being measured. Now we are in a position to compare these energy differences. If one were to do an absorption experiment comparing the intensities of the same Phillips rotational line used in this experiment and the Swan (1-0) or (0-0) band head, the energy difference obtained would be 11.9 kcal per mole as compared with the values of 16.6 or 11.6 kcal per mole, respectively, obtained in this emission experiment. Thus one would conclude that an absorption experiment would have about the same uncertainty as the experiment reported here.

The relative uncertainty in a determination of the energy difference by an absorption experiment is also dependent on the accuracy with which intensities may be measured. According to the formulae used in Appendix B, the intensity of an emitted feature may be expressed as $I_e = I_b (1 - e^{-bNL})$. Here I_b is the intensity of a black body at the same temperature as the column of gas, b is a constant, N is the concentration of excited gas, and L is the path length of emission. If in the absorption experiment the light from the source is modulated before being passed into the gas and the detector adjusted so that it responds to only this modulated light, then light due to the thermal emission of the gas will not be recorded. In this case the intensity of light at any wavelength after passing through the absorbing column of gas is given by the formula $I = I_0 e^{-bNL}$, where I_0 is the intensity of the source before absorption. From this it follows that $I_a = I_0 - I = I_0 (1 - e^{-bNL})$. The ratio of the height of the absorbed feature to that of the emitted feature is then given by the following relation when the concentrations and path lengths are the same:

$$I_a/I_e = I_0/I_b \,. \qquad (12)$$

Thus we see that the sensitivity of the absorption experiment is the same as that of the emission experiment if the intensity of the source is the same as a black body at the same temperature as the gas. If a source is available yielding a steady intensity corresponding to a brightness temperature greater than the temperature of the gas, then we may measure intensities by absorption with greater precision than by emission. It is assumed that the noise level of the photocell and amplifier does not increase when such an intense light falls on the photocell.

A study of the sources that were available for this purpose was made. A standard General Electric 6-volt tungsten ribbon projection lamp operated at an overloading voltage of 12 volts produced a brightness temperature of 2982°K at a wavelength of 6538 A as determined by an optical pyrometer. However, owing to a decrease in the emissivity of tungsten towards higher wavelengths, the brightness temperature of the lamp at 8960 A the wavelength of the Phillips rotational line, amounts to only 2627°K as calculated by use of the tungsten emissivities presented by de Vos.[8] This temperature is lower than the lowest temperature of the gas at which the Phillips rotational line could first be detected in emission ; therefore if the tungsten lamp were used at this operating voltage the intensities could not even be measured with as much accuracy as in emission. It was felt that overloading the lamp even further would result in too short a lifetime of the lamp for useful purposes.

Another source that was considered was the anode crater of a carbon arc, which according to MacPherson[20] has a brightness temperature of 3820°K at the wavelength of his pyrometer. If we assume an emissivity that does not vary with wavelength at 8960 A, such a source would provide an intensity 5.70 times that of a black body at 2700°K. Thus one could gain in sensitivity by a factor of more than five by performing an absorption experiment using a perfectly steady carbon arc as a source. However, in a preliminary experiment to determine the nature of the carbon arc spectra at this wavelength,

the motion of the point of contact of the arc on the face of the anode produced fluctuations in the recorded intensity amounting to 30% to 50% of the total intensity recorded for the anode. Presumably these fluctuations could be reduced by building an arc to conform to the conditions described by MacPherson, but the fluctuations would have to be reduced to less than one in five hundred to produce a sensitivity in an absorption experiment just equal to that of the emission experiment at 2700°K.

Thus at the present time no suitable source seems to be available for performing an absorption experiment to determine the energy difference between the lower states of C_2 more accurately than that obtained in this emission experiment. A future source for such an absorption experiment may be a tantalum carbide filament lamp, which would produce a brightness temperature of well over 3000°K with the steadiness in intensity that is required for this experiment.

Comparison with Previous Work

Now let us compare the value for the heat of formation of the $^3\Pi_u$ state of C_2 determined in this experiment with that obtained by Krikorian. He gives a value of 191.4 ± 5 kcal, but this value must be corrected for the calibration of his pyrometer and the recent revision in the heat of sublimation of Zr. (See Appendix A.) We obtain for his corrected heat a value of 194.1 ± 5 kcal per mole; the change in his heat is small since his heat was based on a measurement of the comparatively small difference in energy between emitting levels of Zr and C_2. Most of the correction is due to the different heat of sublimation of Zr used. This value should be compared with the value 203 ± 4 kcal per mole obtained in this work; it may be seen that these values barely agree within experimental error. It is felt that the heat of sublimation of C_2 obtained in this work is as reliable as that of Krikorian, even though it is based on the measurement of the total heat of formation instead of a comparatively small difference between two heats. The reason for this evaluation is that the discrepancy in the heat of formation determined by using different heating tubes is about the same

in this experiment as in that by Krikorian; however, the heat in this work is based on many more runs with different heating tubes than in that of Krikorian.

The cause of part of the discrepancy between the two values may be found in the self-absorption corrections. Krikorian's self-absorption corrections added 11.9 kcal to his heat of formation of Zr, and 7.2 kcal to his heat of sublimation of C_2. For reasons discussed in Appendix D I believe that his corrections for the Swan (1-0) band and probably for the Zr feature are too high. Thus the self-absorption corrections in Krikorian's work were adjusted to agree with the ones used in this work. The result of this adjustment was that Krikorian's Zr heat was lowered by 6.8 kcal and his C_2 heat by 4.1 kcal.

Krikorian obtained his value for the heat of sublimation of C_2 by measuring the difference in energy between the emitting levels of Zr and C_2 and subtracting this value from the heat of formation of the particular state of Zr that was responsible for the emitted line. Thus the heat that he quotes for C_2 should be raised by the difference between the two corrections mentioned at the end of the preceding paragraph.

Krikorian's heat is then corrected to 196.8 ± 5 kcal per mole, as compared with the value obtained in this experiment of 203 ± 4 kcal per mole. These two independent measurements agree well within experimental error, and it seems reasonable to average these two results to obtain the best heat so far determined by measuring the temperature coefficient of C_2 spectral intensities. Thus we obtain, for the heat of sublimation of C_2 from graphite at $0^\circ K$, $\Delta H_0^\circ = 200 \pm 5$ kcal per mole. It is unlikely that a more accurate value for this quantity will be determined by use of methods that depend on temperature coefficients. The determination of a more precise value for the heat of sublimation of C_2 thus awaits the direct measurement of the absolute "f" value for the Swan system; then the third law of thermodynamics may provide this heat with greater certainty.

The value arrived at above for the heat of sublimation of C_2 gas agrees well with the results obtained from mass spectroscopic work presented previously: 202 ± 20 kcal by Honig[15] and 197 ± 7 kcal by Chupka and Inghram.[5] Since the mass spectroscopic data do not depend on which state of C_2 is the ground state of the molecule, this agreement may be considered as evidence for the assumption that no unobserved energy state of C_2 is lower in energy than the $^3\Pi_u$ state. Using the limits set on their value by Chupka and Inghram and the limits set on the value for the heat of formation of the $^3\Pi_u$ state given above, we may conclude that no state of C_2 could be lower than the $^3\Pi_u$ state by more than 15 kcal or 0.6 ev.

Dissociation Energy and Electronic Energy Levels of C_2

If we assume the $^3\Pi_u$ state is the ground state, we may now evaluate the dissociation energy of the C_2 molecule. This may be defined as the heat at 0°K of the reaction

$$C_2 \text{ (gas)} = 2 \text{ C (gas)}. \qquad (13)$$

We obtain this value by subtracting ΔH_0^o of Reaction (2),

$$2 \text{ C (graphite)} = C_2 \text{ (gas)}, \qquad (2)$$

from twice the value of ΔH_0^o for the reaction

$$\text{C (graphite)} = \text{C (gas)}. \qquad (14)$$

The best value of the heat of sublimation of monatomic carbon at 0°K is given by Brewer and Searcy as 169.58 ± 0.45 kcal per mole.[3] Thus we obtain a value for D_0, the heat of dissociation of C_2, of 139.2 ± 5 kcal per mole or 6.04 ± 0.22 ev per molecule.

Gaydon,[12] using a linear Birge-Sponer extrapolation of the assumed ground state, $X\,^3\Pi_u$*, of C_2, obtained an upper limit of

*The letter designations used in this section for the observed states of C_2 are those used by Herzberg.[14]

7.0 ev for this D_0 of C_2. Phillips,[26] using a linear extrapolation of the $\underline{A}\,^3\Pi_g$ state, obtained three possible upper limits on this quantity of 5.30, 4.04, and 2.62 ev, corresponding to the assumptions that the state dissociates to give an atom of carbon in the ground state of the atom (^3P) plus a second atom in the ^3P, ^1D, or in the ^1S state. The value obtained in this work for D_0 definitely points to two ^3P atoms as the products of dissociation of this state, but is above Phillips's upper limit by an amount that is greater than the combined uncertainties in the values. This might be explained by the assumption of a slight inflexion in the $\Delta G_{v+1/2}$ versus $\underline{v}$ curve for this state, yielding positive curvature in this curve beyond the highest observed vibrational quantum. Such inflections have been observed for the excited states of some molecules.

From the measured energy difference between the lowest vibrational levels of the $^3\Pi_u$ and the $^1\Sigma_g^+$ states and the observed transitions for C_2 we may now calculate the heights of all the observed electronic levels of C_2 above the $^3\Pi_u$ state. Furthermore we may try to predict the positions of the as-yet-unobserved low-lying states of C_2 by revising Mulliken's predictions. Mulliken[24] in 1939 published a paper in which he estimated the heights of the energy levels of C_2 on the basis of their molecular orbitals and the electronic transitions of C_2 and similar molecules which had been observed at that time. He also used an emperical formula for calculating r_0 values for the different states. Since that time two new transitions, including one new state of C_2, have been observed.[11,25] Therefore Mulliken's prediction that in the molecular orbital configuration, $\sigma_g{}^2\sigma_u{}^2\pi_u{}^3\sigma_g$, the $\underline{b}\,^1\Pi_u$ state lies 1.6 ev above the $\underline{X}\,^3\Pi_u$ state was retained; the mean energy of the $\sigma_g{}^2\sigma_u{}^2\pi_u{}^3\sigma_g$ configuration was altered from 0 ev to minus 0.2 ev with respect to the other configuration on the basis of the Phillips transition. This revision leads to a prediction that the potential minimum of the $\underline{a}\,^1\Sigma_g^+$ state lies 0.6 ev above the same for the $\underline{X}\,^3\Pi_u$ state; this should be compared with a difference in the minima of 0.34 ± 0.17 ev determined in this work. It is felt that this agreement is satisfactory, considering the nature of the prediction. In addition, the new state discovered by Freymark may be

assigned the configuration $\sigma_g^2\pi_u^4\sigma_g^2$ on the basis of its energy (predicted 6 to 7 ev, observed 7.08 ev). Its internuclear distance was predicted on the basis of Mulliken's formula to be 1.12A; the value for this quantity observed by Freymark was 1.258A. However, the agreement between predicted and observed internuclear distance obtained by correlating this state with any other $^1\Sigma_g^+$ state predicted to lie in this energy region is much worse.

In Table III are listed the observed and predicted low-lying energy states of C_2 in order of increasing energy, along with their probable dissociation products. The states that have already been observed are indicated by capital letters for the triplet states and lower-case letters for the singlet. The molecular orbitals to which each state belongs is indicated by a letter in the appropriate column as follows:

(a) Stands for $\sigma_g^2\sigma_u^2\pi_u 4$;

(b) $\sigma_g^2\sigma_u^2\pi_u^3\sigma_g$;

(c) $\sigma_g^2\sigma_u^2\pi_u^2\sigma_g^2$;

(d) $\sigma_g^2\sigma_u\pi_u^4\sigma_g$;

(e) $\sigma_g^2\sigma_u\pi_u^3\sigma_g^2$;

(f) $\sigma_g^2\sigma_u^2\pi_u^3\pi_g$;

(g) $\sigma_g^2\sigma_u^2\pi_u^2\sigma_g\pi_g$;

(h) $\sigma_g^2\sigma_u^2\pi_u\sigma_g^2\pi_g$ and

(i) $\sigma_g^2\pi_u^4\sigma_g^2$.

The observed energies presented in the table are calculated from the observed electronic transitions and the difference in the potential minima for the $\underline{a}\ ^1\Sigma_g^+$ and the $\underline{X}\ ^3\Pi_u$ states measured in this work.

The predicted energies were obtained by adjusting the mean energy of each molecular orbital configuration to correspond to the energies determined for the observed states that arise from that configuration. Where no energy level of a particular configuration had been observed the mean energies predicted by Mulliken were retained. These mean energies are subject to further revision as additional states are observed. The spread in energy allowed for the states in each configuration corresponds to that used by Mulliken, and usually amounts to no more than 2 ev.

Values of r_0 the internuclear distance for the zero vibrational level, predicted by using Mulliken's empirical formula, are presented for each state for help in identifying newly observed levels and for the purpose of predicting the appearance of possible transitions between the predicted states. The constants in the formula were revised to take into account more recent values obtained for the r_0's of Configurations (b) (e) and (g) on which the formula is based.

The probable atomic dissociation products for each state are presented in the next to the last column. These products were arrived at by using the rules summarized by Gaydon[12] for correlating atomic and molecular states, i.e., the combination of two atoms in certain atomic states can produce a molecule in only certain predictable states and Hund's noncrossing rule, which states that the potential-energy curves of two states of the same type cannot cross, was also used. The dissociation energy D_e of each state of C_2 could then be calculated, since the dissociation energy for the ground state is known and the relative energies of combinations of atoms in different states may be obtained from Moore's tables.[23] These energies are presented in the last column.

In addition to the lower-lying levels shown in Table III one finds that several additional molecular states may be predicted to arise from two unexcited carbon atoms ($^3P + {}^3P$). Since, according to Mulliken's predictions, no such states may have energies less than 8 ev, one would expect these states to be highly repulsive in nature. These states are as follows: $^5\Sigma_g^+$ (2), $^5\Sigma_u^-$, $^5\Pi_u$, and $^5\Delta_g$.

Table III

Predicted and observed low-lying energy levels of the C_2 molecule listed in order of increasing predicted energy. The observed and predicted internuclear distances and the expected dissociation products and energies are also listed for each state.

Obs. state des.	Type of state	Molec. orb. des.	Observed energy, Te (ev)	Predicted energy, Te (ev)	Obs. r_0 (A)	Pred. r_0 (A)	Dissoc. products	Dissoc. energy, D_e (ev)
X	$^3\Pi_u$	b	0.00		1.317	(1.32)	$^3P+^3P$	6.05
a	$^1\Sigma_g^{+*}$	a	0.34		1.245	1.23	$^3P+^3P$	5.71
	$^3\Sigma_g^-$	c		0.5		1.41	$^3P+^3P$	5.6
	$^1\Delta_g^*$	c		1.0		1.41	$^3P+^3P$	5.1
b	$^1\Pi_u$	b	1.38		1.322	(1.32)	$^3P+^3P$	4.67
	$^1\Sigma_g^+$	c		1.5		1.41	$^3P+^3P$	4.6
A	$^3\Pi_g$	e	2.39		1.269	(1.27)	$^3P+^3P$	3.41
	$^3\Sigma_u^+$	d		3.5–4.5		1.20	$^3P+^3P$	1.5–2.5
c	$^1\Pi_g$	e	4.59		1.278	(1.27)	$^3P+^3P$	1.31
B	$^3\Pi_g$	g	4.97		1.543	(1.54)	$^3P+^1D$	2.34
d	$^1\Sigma_u^+$	d	5.70		1.241	1.20	$^1D+^1S$	4.29
	$^3\Sigma_u^+$	f		5–6.5		1.45	$^3P+^3P$	-0.5–1
	$^1\Sigma_u^+$	f		5–6.5		1.45	$^1D+^1S$	3.5–5

Table III(continued)

	$^3\phi_g$ *	g		5-6.5		1.54	$^3P+^1D$ 1-2.5
	$^1\phi_g$ *	g		5-6.5		1.54	$^1D+^1D$ 2-3.5
	$^5\Pi_g$ *	g		5-6.5		1.54	$^3P+^3P$ -0.5-1
	$^3\Sigma_u^+$	h		5-6.5		1.63	$^3P+^1D$ 1-2.5
	$^1\Sigma_u^+$	h		5-6.5		1.63	$^1D+^1S$ 3.5-5
e	$^1\Sigma_g^+$	i	7.08		1.258	1.14	$^1D+^1D$ 1.49
	$^3\Delta_u$	f		6-7		1.45	$^3P+^3P$ -1-0
	$^1\Delta_u$	f		6-7		1.45	$^1D+^1D$ 1.5-2.5
	$^3\Pi_g(2)$	g		6-7		1.54	$^3P+^1D$ 0.5-1.5
	$^3\Pi_g$	g		6-7		1.54	$^3P+^1S$ 2-3
	$^3\Delta_u$	h		6-7		1.63	$^3P+^1D$ 0.5-1.5
	$^1\Delta_u$	h		6-7		1.63	$^1D+^1S$ 3-4
	$^3\Sigma_u^-$	f		6.5-8		1.45	$^3P+^1D$ -0.5-1.5
	$^1\Sigma_u^-$	f		6.5-8		1.45	$^3P+^3P$ -2- -0.5
	$^1\Pi_g(2)$	g		6.5-8		1.54	$^1D+^1D$ 0.5-2
	$^1\Pi_g$	g		6.5-8		1.54	$^1D+^1S$ 2-3.5
	$^3\Sigma_u^-$	h		6.5-8		1.63	$^3P+^1D$ -0.5-1
	$^1\Sigma_u^-$	h		6.5-8		1.63	$^3P+^3P$ -2- -0.5

*Metastable states

It should be kept in mind that the mean energies of any configurations presented in Table III are subject to an uncertainty of at least one electron volt when no states of that configuration have yet been observed. Therefore although the low-lying states of Configuration (c) $^3\Sigma_g^-$, $^1\Delta_g$, and $^1\Sigma_g^+$, have been assigned energies of 0.5, 1.0, and 1.5 ev respectively, in Table III they could have energies as low as -0.5, 0.0, and 0.5 ev with respect to the $\underline{X}\,^3\Pi_u$ state. At this point one might ask why have not strong transitions been observed for these states if these states were this low in energy? We may find the answer by considering the possible strong transitions that might occur between the low-lying states listed in Table III. Such strong transitions must, for C_2, obey the selection rules presented by Gaydon: for case $\underline{a}$ and $\underline{b}$ coupling $\Delta\Lambda = 0, \pm 1$; $\Delta S = 0$ (i.e., no change in multiplicity); $\underline{g}$ states may combine with $\underline{u}$ states, but two $\underline{g}$ or two $\underline{u}$ states cannot combine; and finally states with like sign may undergo transitions, but not with unlike sighs in the case of Σ states. In this way we find that there could be no strong transitions between the states of Configuration (c) and other states of Table III in the visible or air ultraviolet regions. Transitions to states not listed in this table would lie at least as far out as the vacuum ultraviolet region.

Thus, although we may be reasonably sure that the $\underline{X}\,^3\Pi_u$ state is the ground state of C_2, we must still consider the possibility that the $^3\Sigma_g^-$ or $^1\Delta_g$ state may be lower in energy. It is here suggested that the position of these levels could be determined with precision by finding transitions in the infrared region between them and the low-lying observed states. On the basis of Table III we may predict three such transitions: $\underline{X}\,^3\Pi_u$ to $^3\Sigma_g^-$ with its (0-0) band at approximately 4000 cm^{-1}, $^1\Delta_g$ to $\underline{b}\,^1\Pi_u$ at 2400 cm^{-1}, and $\underline{b}\,^1\Pi_u$ to $^1\Sigma_g^+$ at about 1600 cm^{-1}. All three of these transitions would be expected to have moderately well-formed band heads and wide parabolic distributions of intensities among the various vibrational bands similar to the Phillips transition ($\underline{a}$ to $\underline{b}$); the predicted change in internuclear distance is about the same as that which occurs in this observed transition. One might find these transitions by using an equilibrium thermal source, a discharge

through hydrocarbon vapor or a carbon arc in either emission or absorption. If any one of the three transitions were found, the energies of all three states of Configuration (c) would be determined relatively well, for the predicted relative energies of the three states should be quite accurate.

Another object in searching for transitions between the states of Table III might be to find a transition in which the discrete band structure converges to a continuum in a region where the transition still has appreciable intensity. If such a transition were observed between two states, at least one of which has been already observed, one could obtain a precise dissociation energy for the ground state of the C_2 molecule from the convergence limit for the system. Thus a value for the heat of formation of C_2 gas would be obtained which would be much more accurate than any value that can be obtained from thermochemical measurements. According to Gaydon, a transition having the desired properties might occur in absorption between two states, the lower of which is stable and the upper of which has a shallow potential-energy curve which is displaced somewhat to greater internuclear distances than the lower. On examining Table III we find several possible transitions that might have such properties. Some examples are $\underline{A}\ ^3\Pi_g$ to $^3\Sigma^+_u$, $^3\Delta_u$, and $^3\Sigma^-_u$ with ν_e at from 20,000 to 32,000, 28,000 to 36,000, and 32,000 to 44,000 cm^{-1}, respectively. These transitions might be found in the absorption spectrum of the King furnace or a discharge if the strong ultraviolet continuum of the high-pressure xenon arc lamp or the hydrogen arc lamp were used as a background.

A further conclusion at which we might arrive from an examination of Table III is that the position of the low $^3\Sigma^-_g$ state supports Gaydon's explanation of the high-pressure bands of C_2.[12] These bands arise from the $v = 6$ level of the $\underline{A}\ ^3\Pi_g$ state of the Swan bands, and have an abnormally high intensity under certain excitation conditions. Herzberg assumes that this high intensity is produced by a collision of atoms that produce C_2 in this state; thus he arrives at a dissociation energy for C_2 of 3.6 ev.[14] However, Gaydon mentions that the abnormal intensity may correspond to a radiationless transition from another stable state,

which is selectively excited, to the v = 6 level of the $\underline{A}\ ^3\Pi_g$ state; thus he concludes that the dissociation energy may be much higher than 3.6 ev. In Table III we see that the potential energy curve of the $^3\Sigma_g^-$ state may lie in such a position that it would intersect the $\underline{A}\ ^3\Pi_g$ state at the v = 6 vibrational level. This is the only state near the upper state of the Swan bands that could undergo a radiationless transition to this state. The possibility of the intersection of the curves is even greater if we remember that the mean energy of Configuration (c) is uncertain by as much as 1 ev.

Figure 8 is a chart of all the transitions that one might predict from consideration of every pair of terms in Table III between which a transition might occur in the ultraviolet, visible, or infrared regions of the spectrum of C_2. Solid lines represent discrete band systems; dashed lines, systems that may be continuous or discrete; and dotted lines, continuous transitions. The excitation of the higher state of each transition has been included as a guide in predicting the best source for the production of each band system. The uncertainty in the predicted ν_e's of Fig. 8 amounts to ± 6000 cm^{-1} in most cases.

Phillips and Brewer[28] describe a strong ultraviolet continuum with maxima at 4000 and 4300 A as appearing in the King furnace spectrum at over 2500°C. They found that the intensity of the continuum at 4000 A varied as the third power of the monatomic carbon pressure, and thus attributed the continuum to the C_3 molecule. Assuming that this continuum represents the dissociation of the C_3 molecule to the lowest possible energy possible energy products, $C_2(^3\Pi_u)$ and C (^{3}P), and using the value found by Thorn and Winslow[36] for the heat of formation of C_3 from solid graphite, 8.0 ev, one may calculate that the state responsible for this continuous emission is excited by 8.1 ev. It seems unlikely that such a transition of the C_3 molecule could account for the total intensity observed for the continuum, which according to Phillips and Brewer has a total integrated intensity at 2700°C equal to that for all the Swan bands. For the C_2 molecule the most highly excited transition that has been observed in the King furnace is the Swan transition with its highest state at

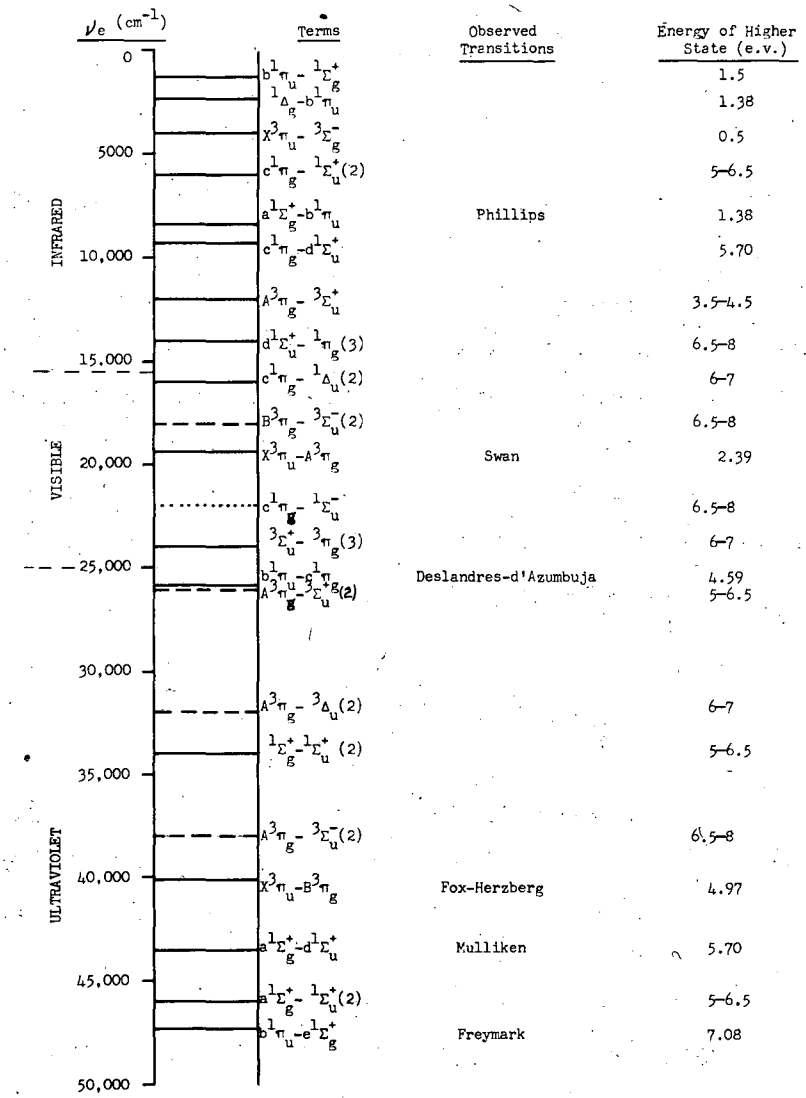

Fig. 8. Chart of predicted and observed transitions of the C_2 molecule. Solid lines represent discrete systems; dashed, possibly continuous or discrete; dotted, continuous. The excitation of the higher state is also included.

only 2.39 ev. Therefore it seems likely that some other molecule than C_3 is partly responsible for this continuum. From an inspection of Fig. 8 one finds several possible continuous transitions of the C_2 molecule predicted for this wavelength region. Indeed, one of these transitions might account for the maximum observed in the continuum at 4300 A.

Absolute f values for the Swan and Phillips Transitions

Using the absolute intensities of the Swan and Phillips transitions measured in this work for the purpose of ascertaining the degree of self-absorption, one may calculate the absolute f values of the vibrational bands of the Swan and Phillips systems. Let us consider the relative intensities of the rotational lines in a branch of a vibrational band to be proportional only to the populations of the rotational levels giving rise to those lines. Then we may define the f value for that particular band in a manner similar to that of an atomic line as presented in Mitchell and Zemansky,[21]

$$\int_0^\infty k_\nu d\nu = \frac{\pi e^2}{mc} N_{J''} f_{v'v''} . \qquad (15)$$

Here k_ν is the absorption coefficient of the rotational lines that arise from the J'' level, $N_{J''}$ is the concentration of molecules in the rotational level, and $f_{v'v''}$ is the absolute f value for the $(v'-v'')$ transition.

In Appendix B quantities Q_ν and R_ν were defined so that $Q_\nu R_\nu = b_\nu NL$; however, $b_\nu N$ is simply the commonly used absorption coefficient k_ν. Now, in a Doppler-broadened line,

$$\int_0^\infty k_\nu d\nu = 1/2\, k_0\, \Delta\nu_D \sqrt{\pi/\ell n\, 2}$$

where k_0 is the absorption coefficient at the peak of the line and $\Delta\nu_D$ is the Doppler width of the line and is given by the expression $2\sqrt{2R\,\ell n\, 2}/c\ \nu_0 \sqrt{T/M}$. For the Swan (1-0) band head the QR values for the band

head are presented in Table VII of Appendix D; the ratio of this quantity to Q_0R_0 at the peak of a triplet component in the P branch was calculated by the methods used in constructing Fig. 9. Thus from the Q_0R_0 value of its peak and the path length of the column of gas the integrated absorption coefficient for a particular triplet component was calculated:

$$\int_0^\infty k_\nu \, d\nu = \frac{Q_0R_0}{2L} \, \Delta\nu_D \sqrt{\pi/\ell n 2} \, . \qquad (16)$$

To obtain the total integrated absorption coefficient for all the components arising from that particular J'' rotational level, this value was multiplied by six to account for the three components in each of the two branches present.

The path length $\underline{L}$ had to be estimated for use in Eq. (16). The heating tubes used in the intensity measurements were of such a design that there was a 15.2-cm heating zone at the center of the tube with comparatively thin walls. At each end of the heating zone there was an abrupt increase in wall thickness, which produced sharp temperature gradients. If we allow 1 cm at each end of the heating zone as the depth of penetration of the steep gradient, then we are left with 13 cm path length of quite uniform temperature. If we allow for a possible 30°K temperature gradient in this uniform heating zone, and if the temperature reading of the hottest part of the zone is used, then the effective path length is decreased still further by 2 cm. Since this is the maximum temperature gradient occurring in these intensity measurements, a path length of 13 ± 2 cm was used in the calculations. This relative uncertainty is greater than the variation in the absolute intensities measured by use of different heating tubes.

By using the $(F^\circ - H_0^\circ)/T$ value calculated for C_2 at 3000°K by means of spectroscopic data, the $(F^\circ - H_0^\circ)/T$ value for solid graphite, and the heat of formation of C_2 decided on in this work, one may calculate the pressure of C_2 gas at this temperature. To calculate the total pressure of C_2 gas at 3000°K one would have to include in his calculation of $(F^\circ - H_0^\circ)/T$ the contribution of all low-lying electronic

states of C_2, i.e., $\underline{a}\ ^1\Sigma_g^+$ and possibly $^3\Sigma_g^-$ as well as $\underline{X}\ ^3\Pi_u$. However, in calculating the absolute $\underline{f}$ value for the Swan bands, we are concerned only with the population of the $\underline{X}\ ^3\Pi_u$ state; thus the calculations of previous investigators who considered only this state may be used for this purpose. For $-(F^\circ - H_0^\circ)/T$ at 3000°K for C_2, Gordon,[13] obtains a value of 59.666 eu corresponding to a degeneracy of $3(2J + 1)$ for each rotational level; Kelley[16] gives a value of 58.238 eu, corresponding to a degeneracy of $3(2J + 1)/2$ for each level. The correct degeneracy for the $^3\Pi_u$ state is obtained by multiplying the rotational degeneracy $(2J + 1)$ by 3 to account for the spin multiplicity, and then by 2 because of lambda doubling, and finally dividing the product by 2, since half the levels are missing owing to the twofold symmetry of C_2. Thus the value given by Gordon is the correct one.

For solid graphite at 3000°K, $-(F^\circ - H_0^\circ)/T$ equals 7.28 eu, according to the National Bureau of Standards;[32] for the heat of vaporization of C_2 at 0°K the value 200 ± 5 kcal was used. These values lead to a pressure of C_2 gas in the $\underline{X}\ ^3\Pi_u$ state of 1.91×10^{-5} atmos. A factor of two uncertainty in pressure is due to the uncertainty quoted for the heat of vaporization. By use of the ideal gas law the concentration of C_2 molecules per cc may be calculated.

Now that we know the total concentration of C_2 molecules in the $^3\Pi_u$ state, we may find the concentration in the particular $\underline{J}$ level of that state by using the formula

$$\frac{N_J}{N} = \frac{3(2J + 1)\, e^{-hcB_v J(J+1)/kT} e^{-\omega_0 v}}{Q_{rot}\ Q_{vib}}, \qquad (17)$$

where Q_{rot} is the rotational-state sum and is given to a close approximation by the expression $3kT/hcB_v$; Q_{vib} is the vibrational-state sum.

Thus the quantities $\int_0^\infty k_\nu' d\nu$ and $N_{J''}$ calculated for a particular rotational level of the Swan (1-0) band were substituted into Eq. (15) and an $\underline{f}$ value of 8.1×10^{-3} was obtained for this band. King made absolute intensity measurements on the Swan (0-0) band.

These yield an f_{00} value of 1.29×10^{-2} based on a pressure of C_2 calculated using the ΔH_0° of vaporization decided on in this work. Using the relative $\underline{f}$ values for the Swan bands tabulated by Fraser, Jarmain, and Nicholls,[10] we may obtain an f_{10} value of 4.2×10^{-3} from King's intensity measurement.

If we consider that the $\underline{f}$ value for the total electronic transition is simply the sum of all the $\underline{f}$ values for vibrational bands arising from a single vibrational level, then, using the relative $\underline{f}$ values of Fraser, Jarmain and Nicholls and an f_{10} of 8.1×10^{-3}, we obtain an $\underline{f}$ value for the total Swan transition of 0.034. These experimental $\underline{f}$ values are uncertain by a factor of two due to the 5 kcal uncertainty in the heat of formation of C_2. This may be compared with values calculated from quantum mechanical theory by Shull[33] and by Stephenson.[34] Shull obtained a value of 0.18 for the Swan transition. Stephenson calculated 0.029, but ignored hybridization of orbitals.

From the R_0 values of the Phillips rotational line presented in Table VI of Appendix C and the pressure of C_2 gas in the $\underline{a}\ ^1\Sigma_g^+$ state, one can calculate an absolute $\underline{f}$ value for the (2-0) Phillips band in the same manner as for the Swan band. To compute the total integrated absorption coefficient for all the lines rising from a given rotational level one must multiply the absorption coefficient of a single rotational line in the $\underline{Q}$ branch by 2, since the lines of the $\underline{Q}$ branch have twice the intensity of the corresponding lines in the $\underline{P}$ or $\underline{R}$ branch. In calculating free-energy functions or rotational-state sums for the $\underline{a}\ ^1\Sigma_g^+$ state, it must be remembered that the degeneracy of each level is simply $\underline{2J + 1}$, since there is no lambda doubling and the spin multiplicity is only 1; however, all the odd-numbered levels are missing owing to the twofold symmetry of the C_2 molecule.

The $\underline{f}$ value of the Phillips (2-0) band was actually calculated relative to that for the Swan (1-0) band, since the relative $\underline{f}$ values do not depend on the rather inaccurately known heat of formation of C_2 gas and the path length involved in the measurements. In this way the $\underline{f}$ value for the Phillips (2-0) band was found to be smaller than that for the Swan (1-0) band by a factor of 0.468 ± 0.028. This leads to

an absolute $\underline{f}$ value for the Phillips (2-0) band of 3.8×10^{-3}; this value is uncertain by a factor of two or three. Accurate relative $\underline{f}$ values for the different vibrational bands of the Phillips transition are not yet known, but one might estimate that the total $\underline{f}$ value for the transition would be about three and one-half times that of the (2-0) band, on the basis of the observed band intensities, and thus equal to 0.012. No theoretical values for this quantity have yet been reported.

ACKNOWLEDGMENTS

I am deeply indebted to Professor Leo Brewer for the guidance needed to carry out this project. His inexhaustable patience and sharp insight were a great inspiration to me.

I also wish to thank Professor Francis A. Jenkins, who provided much of the spectroscopic equipment used in this work. Professor John G. Phillips built and helped maintain the photometric equipment. The advice and guidance provided by both these men is deeply appreciated. Dr. Oscar H. Krikorian also presented many useful ideas.

This work was done under the auspices of the U.S. Atomic Energy Commission.

APPENDIX

A. Temperature Scale

In view of the discrepancies obtained with the National Bureau of Standards corrections for No. 3 pyrometer and the intercomparison of Nos. 2 and 3, an independent calibration of pyrometer No. 2 was made. First the "H" scales of Nos. 2 and 3 were calibrated by sighting the pyrometers on a standardized General Electric lamp No. 86-P-36, whose current-versus-temperature calibration had been supplied by General Electric in 1946. This calibration was first corrected to the 1948 thermodynamic scale.[6] The corrections for both pyrometers appeared to be the same within experimental error, 1° or 2°, through the whole scale range, 1100° to 1750°C. The discrepancy between these corrections and those of the Bureau of Standards varied from 0° to 6° through most of this range; thus the discrepancy for the "H" range is rather small.

Once the "H" scale calibration is known one can calculate the corrections for the "xH" range by using the ratio of the transmissions of the "H" and "xH" filters according to the methods given by Forsythe.[9] The relationship between the true brightness temperature of an object, T_1 (in degrees Kelvin) and the temperature observed with the pyrometer with a filter located between the filament of the pyrometer and the object T_2 is given by

$$1/T_1 - 1/T_2 = \lambda_e/c_2 \ln P = K . \qquad (18)$$

Here λ_e is the effective wavelength of the pyrometer, c_2 is a constant with value 1.438 cm-deg, and $\underline{P}$ is the integrated transmission of the filter. For the purpose of calibrating the "xH" scale from the already calibrated "H" scale, $\underline{P}$ is defined as

$$P = \frac{\Sigma\, J(T_1)\, S\, p_r\, p_{xH}}{\Sigma\, J(T_1)\, S\, p_r\, p_H} , \qquad (19)$$

where $J(T_1)$, is the Wien's law expression, S is eye sensitivity, p_r is the transmission of the monochromatic filter, and p_{xH} and p_H are the transmissions of the "xH" and "H" filter screens at a certain wavelength. The terms of the summation are taken at 50-angstrom intervals throughout the wavelength region in which they make an appreciable contribution.

The effective wavelength λ_e to be used in Eq. (18) is precisely defined as the wavelength at which this relation holds:

$$\frac{J(T_1)_\lambda}{J(T_2)_\lambda} = \frac{\Sigma J(T_1)\, S\, p_r\, p_{xH}}{\Sigma J(T_2)\, S\, p_r\, p_{xH}} . \qquad (20)$$

However, at the high temperatures and with the temperature intervals used in applying Eq. (18) to the calibration of the "xH" scale of the pyrometer, this exact effective wavelength for the temperatures T_1 and T_2 is represented to a close approximation (1 in 6000) and with much less effort by the limiting effective wavelength of the temperature $(T_1 + T_2)/2$. The limiting effective wavelength λ_e^o obtained for a temperature $\underline{T}$ from Eq. (20) by taking smaller and smaller intervals around $\underline{T}$ until the resulting value of λ_e calculated no longer changes. At the high temperatures used in this calibration, an interval of 500^o was small enough to yield λ_e^o with an accuracy of 1 in 6000. Since the "H" and "xH" filters are not quite neutral through this wavelength region, slightly different values of λ_e^o are obtained from Eq. (20) when p_H is substituted for p_{xH}. Therefore the average of these values was used in Eq. (18). The variation of λ_e^o with T is quite small, only about 0.0107 A per degree.

In order to obtain the variation in transmission of the different filters with wavelength, light passing through them from a constant-temperature tungsten filament was scanned with a 1P-28 photomultiplier in the wavelength region of interest. The monochromatic, "H", and "xH" filter screens of Pyrometer-2 and the light source itself were scanned; the conditions of the experiment were not such as to lead to the absolute ratio of the integrated transmission of the "H" and "xH" filters.

To obtain the absolute transmission ratio Pyrometer-2 was sighted on a tungsten-band lamp at a brightness temperature of about 1600°C with the "H" filter in place and the temperature read on the "H" scale. Then with the lamp at the same temperature but with the "xH" filter in place, the temperature reading on the calibrated "H" scale was recorded again. These temperatures, when corrected and substituted in Eq. (18), gave $\underline{K}$ values for the different lamp temperatures. The average value of $\underline{K}$ thus found was $-(1.686 \pm 0.011)\ 10^{-4}$ deg.$^{-1}$ at $T_1 = 1877°K$. The uncertainty shown in $\underline{K}$ is the average deviation of five determinations of $\underline{K}$ at temperatures centered around 1877°K; this rather large uncertainty is due to the difficulty in reading temperatures at the ends of the scale regions, where judgment of intensities is poor.

From this value of $\underline{K}$ the value of $\underline{P}$ of Eq. (1.8) could be determined. Then $\underline{P}$ was calculated at other temperatures by using the measured variation of transmission with wavelength and Eq. (19). These figures in turn, with the λ_e^o calculated for $(T_1 + T_2)/2$, yielded $\underline{K}$ at other temperatures T_1 along the "xH" scale. Although the absolute value of the $\underline{K}$'s thus calculated is uncertain, the relative values of $\underline{K}$ at different temperatures should have an accuracy of better than 1 in 6000.

For Pyrometer No. 2 the values of $\underline{K}$ for different values of T_1 and T_2 thus calculated are presented in Table IV along with the quantities $\underline{P}$ and λ_e^o used in calculating them. Also presented for comparison are values of $\underline{K}$ for Pyrometer No. 2 calculated by using readings that appear adjacent to each other on the "H" and "xH" scales of No. 2 and adjusted according to the corrections supplied by the NBS for the respective scales of No. 3 and the intercomparison of the two instruments.

Table IV

Calculated transmissions, effective wavelengths, and the resulting scale constants for Pyrometer No. 2. Also presented are the scale factors obtained from the NBS calibration of Pyrometer No. 3 and the intercomparison of the two instruments.

T_1 (^oK)	T_2 (^oK)	$P \times 10^2$	- log P	λ_e (A)	$-K \times 10^4$ (deg.$^{-1}$) (from P)	$-K \times 10^4$ (deg.$^{-1}$) (NBS)
2000	1496	2.476	1.6062	6554	1.686	1.695
2250	1631	2.468	1.6077	6551	1.687	1.698
2500	1758	2.460	1.6091	6548	1.687	1.680
2750	1878	2.453	1.6103	6545	1.688	1.674
3000	1992	2.449	1.6110	6543	1.688	1.652
3250	2099	2.445	1.6117	6540	1.688[a]	1.626[b]

[a] A value of 1.689×10^{-4} deg.$^{-1}$ was calculated at this temperature by using Planck's law in place of Eq. (18). The use of Planck's law is specified for the 1948 thermodynamic scale, but this correction is negligible at the highest temperature used here.

[b] This value is extrapolated from the values at lower temperatures.

It may be seen that the variation with temperature of the value of $\underline{K}$ calculated from the measured transmissions disagrees in both size and direction with the variation of $\underline{K}$ obtained from the Bureau of Standards corrections. The calculated $\underline{K}$ remains almost constant, since the variation in log P almost cancels the variation in λ_e. The only reason that $\underline{P}$ varies at all is that the ratio of the transmissions of the "xH" and "H" filters varies slightly with wavelength. In order to obtain a variation in $\underline{K}$ of the order of that given by the Bureau of Standards one would have to assume a large change in the value of $\underline{P}$ with temperature, which seems unreasonable considering the transmissions measured for the filter screens.

The variation of $\underline{K}$ obtained by using the National Bureau of Standards corrections and the scale readings of Pyrometer No. 3 is about the same:

1.673×10^{-4} deg^{-1} at $T_1 = 3000^{\circ}$K to 1.715×10^{-4} deg^{-1} at 2000°K. The original constant used by Leeds and Northrup in manufacturing their scales is $(1.735 \pm 0.001)\ 10^{-4}$ deg^{-1} throughout this range for both pyrometers.

On the basis of these new transmission-constant values and the calibration of the "H" scale of Pyrometer No. 2 made with the General Electric standard lamp, new corrections were calculated for the "xH" scale of this pyrometer. These corrections are tabulated in Table V along with corrections calculated from those given by the Bureau of Standards for Pyrometer No. 3 and the intercomparison of Nos. 2 and 3. These corrections are to be subtracted from the scale reading indicated to obtain the correct temperature in degrees Centigrade.

Table V

Corrections to be subtracted from scale readings of Pyrometer No. 2

Scale reading ($^{\circ}$C)	Corrections from transmissions ($^{\circ}$C)	Bureau of Standards corrections ($^{\circ}$C)
2000	29	19
2200	38	32
2400	48	48
2600	58	73
2800	70	106

When these new corrections are applied to the measurements of Krikorian, his measured heats are corrected by a factor of only 1.0177. We therefore obtain for his measured heat for Reaction (4) a value of 260 as compared with a calculated value of 258.2 kcal based on the measurements by other observers. (See section entitled "Measurement of Temperatures" in text.) The small magnitude of the correction factor might surprise one in view of the rather large corrections given in Table V, since Krikorian used the uncorrected scale readings of Pyrometer No. 2 for his temperatures. This may

be easily understood, however, if one considers that, according to Eq. (18), if one uses a constant value of K throughout the temperature range he will obtain the same difference in reciprocal temperatures as he would with any constant value of K throughout the temperature interval, so long as the "H" scale corrections are the same. Thus when Krikorian accepted the scale readings of the pyrometer directly without any corrections he was in effect applying the original constant value of K used by Leeds and Northrup in manufacturing their scales. Since this new temperature scale, based on the measured transmissions of the various filters and on a calibration of the "H" scale by the General Electric lamp, seems to give the most consistent values for the heats, the temperatures and heats quoted in this thesis are based on this scale.

B. Monochromatic Self-Absorption

For low concentrations of a gas we may say that its intensity of emission at a certain wavelength is directly proportional to the concentration of the excited state that gives rise to the particular transition at this wavelength. However, as the concentration of the emitting gas increases to larger values, we find that the intensity no longer increases as rapidly as the concentration. This phenomen is due to self-absorption. It arises in a column of gas because the molecules that are closer to the observer tend to absorb part of the radiation emitted by the molecules farther away in the column. This effect was found to be present in both the Phillips (2-0) band and the Swan (0-0) and (1-0) bands in the temperature range over which the measurements were made, and therefore the magnitude of these corrections had to be known before accurate heats could be calculated.

The expression for the intensity of emission at a single wavelength as a function of concentration may be easily derived, including the effects of self-absorption. Let us assume that we have a column of emitting gas of uniform cross section and temperature and with length L. If a_ν is a constant representing the intensity of light emitted by a single excited

molecule at a certain wavelength, the intensity emitted by a very thin cross section of the column would be $I_{0\nu} = a_\nu N'_e dx$. Here N'_e is the number of molecules in the excited state of the transition per unit length and dx is the element of length. Now if this cross section is at a distance x down the column from the observer at the end of the column, then the intensity of light reaching the observer from this cross section is given by the Bouguer-Beer equation,

$$I_\nu = I_{0\nu} e^{-b_\nu N x}, \tag{21}$$

where b_ν is the amount of absorption per molecule, and N is the concentration of molecules in the lower state of the transition.

To obtain the intensity emitted by the whole column of gas we sum all the cross sections through the length of the column L,

$$I_\nu = \int_0^L a_\nu N' e^{-b_\nu N x} dx = \frac{a_\nu N'}{b_\nu N} (1 - e^{-b_\nu N L}). \tag{22}$$

This is an exact expression for the intensity of emission as function of the concentrations of the lower and excited states of the transition. The relationship between N' and N is given by the Boltzmann factor:

$$N'/N = e^{-h\nu/kT}.$$

At low concentrations Eq. (22) simplifies. Using a series expansion for the exponent, we obtain

$$I_\nu = a_\nu N' L. \tag{23}$$

Thus at low concentrations one generally assumes linearity between the concentration of excited molecules and the intensity of emission; self-absorption effects begin to appear only when other terms than the first term of the series expansion become important.

At very high concentrations we may draw another conclusion from Eq. (22). As N and N' approach infinity the intensity of the emitted

light must approach that from a black body at the same temperature and wavelength as the column of gas, hereafter signified by $I_{B\nu}$. Thus we see from Expression (22) and the Boltzmann factor that $a_\nu N'/b_\nu N$ must be equivalent to $I_{B\nu}$. Substituting in Eq. (22) we obtain

$$I_\nu = I_{B\nu}(1 - e^{-b_\nu NL}) . \qquad (24)$$

Over much of the temperature range used in this experiment the simple Eq. (23) was adequate. This expression was derived for a single wavelength. However, one may see that there would be a linear relationship between the concentration of the excited state and the integrated emission intensity of any shaped feature where Expression (23) holds at all wavelengths. For example, linearity may be assumed between the intensity of the rotational line of the Phillips band and the concentration of C_2 molecules at low temperatures. We shall assume this line has a Doppler profile, because Krikorian[19] showed that atomic zirconium lines under similar conditions had a Doppler profile; he proved this by making Fabry-Perot measurements on these lines in the King furnace spectrum. When the Phillips rotational line was recorded the instrumental slit widths were many times as wide as the Doppler width calculated for this line. Thus when this feature was traced by the instrument with both its entrance and exit slits the same size, a triangle was recorded with a base equal to twice the slit widths used. The height of this triangle was used as a measure of the integrated intensity of this feature. The intensity thus measured was directly proportional to the concentration of C_2 molecules in the higher state of the transition when the C_2 concentration was sufficiently low.*

*In a Doppler-broadened feature, a_ν changes slightly with temperature at a given wavelength, as evidenced by the fact that the Doppler width--the width of the feature at half intensity--varies with the square root of the absolute temperature. Nevertheless even in this case the area under the curve representing the intensity of the Doppler feature against wavelength--the integrated intensity of the feature--is still directly proportional to concentration. This is obvious if one considers that in this case the intensity of light emitted per molecule is still constant, but simply spread over a greater wavelength region as the temperature increases.

For the Swan-band head, if the instrumental slit width were narrow compared with the unresolved band head, then we could assume that we were making a monochromatic measurement, and therefore Eq. (23) would hold. If the slit widths were large compared with the width of the feature we could assume that the height of the head as recorded on the paper was a measure of the integrated intensity of the feature, and the reasoning of the last paragraph would hold. Since at either extreme there is linearity between the concentration and the recorded height of the feature, this relationship holds in the actual case even though it is probably somewhere between the two extremes.

At higher temperatures deviations from this linear relationship began to show up. Therefore at these temperatures the measured intensities were corrected to yield quantities that vary linearily with the concentration of the molecules in the emitting state. For this purpose a correction factor, which we shall call $\underline{Q}$, may be found such that when it is multiplied by the measured intensity an "ideal" intensity, a quantity which is directly proportional to the concentration of the emitting state, is obtained. This factor is obtained by dividing Eq. (23) by Eq. (24):

$$Q_\nu = \frac{b_\nu NL}{1 - e^{-b_\nu NL}} . \qquad (25)$$

To confirm the validity of this correction factor observe that, using Eq.(22) and Eq.(25), we obtain $Q_\nu I_\nu = a_\nu N'L$, a quantity that is directly proportional to the concentration of molecules in the emitting state.

To evaluate this correction factor experimentally let us use a ratio, the observed intensity of the light emitted from the gas column to the intensity of a black body at the same temperature and wavelength as the column of gas; this ratio can be determined experimentally. Let us call this ratio $\underline{R}_\nu$. We may see how $\underline{R}_\nu$ is related to $\underline{Q}_\nu$ simply by dividing Eq. (24) by $I_{B\nu}$:

$$R_\nu = 1 - e^{-b_\nu NL} . \qquad (26)$$

From this expression readily follows

$$b_\nu NL = -\ln(1 - R_\nu). \tag{27}$$

Thus Q_ν may be given in terms of R_ν,

$$Q_\nu = -\frac{1}{R_\nu}\ln(1 - R_\nu). \tag{28}$$

C. Self-Absorption in the Phillips Rotational Line

From Eq. (28) we may experimentally evaluate the correction factor for a Doppler-broadened line such as the particular Phillips rotational line which we are studying. Here we wish a correction factor for the integrated intensity of the line as recorded by the instrument; however, Eq. (28) applies only to a single wavelength. Therefore we must average this expression over the Doppler profile as follows:

$$Q = \frac{\int_0^\infty Q_\nu I_\nu d\nu}{\int_0^\infty I_\nu d\nu}, \tag{29}$$

where ν is a particular frequency and Q_ν and I_ν are the correction factor and intensity, respectively, at that particular frequency.

In order to obtain a usable expression from the above formula we must make several approximations. The relationship between b_ν, the absorption coefficient at a certain frequency, and b_0, the absorption coefficient at the peak of the Doppler line is given exactly by

$$b_\nu = b_0\, e^{-(2\sqrt{\ln 2}\,(\nu - \nu_0)/\Delta\nu_D)^2}, \tag{30}$$

where $\Delta\nu_D$ is the Doppler width. Now we shall use Eq. (23) as an approximation for I_ν for the purpose of evaluating Q. Remembering that we have $a_\nu N' = b_\nu N I_{B\nu}$, we obtain

$$I_\nu = N L I_{B\nu} b_0 e^{-(2\sqrt{\ell n\, 2}(\nu - \nu_0)/\Delta\nu_D)^2} . \qquad (31)$$

Taking Eq. (28) and making a series expansion for $\ell n\,(1 - R_\nu)$, we find

$$Q_\nu = 1 + \frac{R_\nu}{2} + \frac{R_\nu^2}{3} + \ldots , \qquad (32)$$

where for small values of R_ν the second-order and higher terms may be dropped. These expressions are substituted into Eq. (29) and integrated over all frequencies. It is assumed that $I_{B\nu}$ remains constant over the small frequency range over which I_ν is appreciable. The following simple result is obtained:

$$Q = 1 + \frac{1}{2\sqrt{2}} R_0 . \qquad (33)$$

Here R_0 is the ratio of intensity of the feature to intensity of the black body at the peak of the Doppler line.

The following procedure was used to evaluate this ratio experimentally for the Phillips rotational line. A small graphite plug was placed in the middle of the heating tube so that when the tube was heated the plug was at the same temperature as the gas. Then with the furnace at a constant temperature, light from first the plug and then the emitting gas was trained on the slit of the spectrograph; thus a record was obtained of the intensities of both the feature and the black body at the same wavelength. A Dow-Corning filter No. 3486 was used when the intensity of the black body was measured to prevent second-order light from entering the spectrograph.

Care had to be taken in arranging the optics so that the limiting aperture and the area of the source were the same when the intensities of each of the two sources were being compared. A single lens was placed between the King furnace and the spectrograph in such a position that the graphite plug, which was halfway down the length of the heating tube, was imaged on the face of the spectrograph slit. The distance between the lens and the graphite plug was about 70 cm; between the lens and the slit, 2 m. A small enough stop was placed on the lens so that it was the limiting aperture of the system; a stop was placed on

the slit so that only a small part of the center of the image of the plug or of the emitting gas was allowed to pass through and thus fall on the grating. The lens was moved a short distance in a vertical direction to allow either the image of the plug or that of the gas to fall on the slit stop. Care was taken so that in either case all the light coming through the slit stop fell entirely on the grating surface. Since the column of gas had a finite length, 15 cm, the limiting aperture was not the same for all the light from the emitting gas. At any given stop, the lens subtended a somewhat larger angle for the gas at that end of the heating zone closest to the lens than for the graphite plug, which was halfway down the heating zone. This was balanced out, though, as at the same lens stop the lens subtended a smaller angle for the gas at the rear of the column than for the graphite plug. Thus the optics for the gas and the black-body plug were equivalent.

The value of $\underline{R}_0$ could not be taken directly from the instrumental recording. As mentioned previously the recorded feature was subject to considerable instrumental broadening. However, the area of this recorded feature must be equal to the area of the Doppler-shaped feature that provoked the response. Now, since both slits are the same size, the shape of the instrumentally recorded feature is a triangle whose area is given by the product of I_i, the height of the recorded feature, and $\Delta\gamma_i$, the width of the recorded feature at half intensity. Expressing the equivalence in area of the Doppler-broadened feature and the instrumentally recorded feature, we may say:

$$I_i \, \Delta\nu_i = \int_0^\infty I_\nu \, d\nu = \frac{\sqrt{\pi}}{2\sqrt{\ell n\, 2}} I_0 \, \Delta\nu_D \, . \qquad (34)$$

For I_ν we substitute the expression given by Eq. (34); I_0 is simply the peak intensity of the Doppler feature. Thus we may solve for the actual or Doppler peak intensity in terms of the instrumental peak intensity;

$$I_0 = 0.941 \, \frac{\Delta\nu_i}{\Delta\nu_D} \, I_i \, . \qquad (35)$$

Here $\Delta\nu_D$, the Doppler width, is given by the relationship:

$$\Delta\nu_D = \frac{2\sqrt{2R\ \ell n 2}}{c}\ \nu_0\ \sqrt{T/M}\ . \qquad (36)$$

where $\underline{M}$ is the molecular weight of C_2 and $\underline{c}$ is the velocity of light. I_0 by the measured black-body intensity we obtain the quantity $\underline{R_0}$. When R_0 is substituted into Eq. (33) it gives us the correction factors, which when multiplied by the measured intensities give us intensities which are directly proportional to concentration.

The $\underline{R_0}$ value for the Phillips rotational line, (2-0) band, $J' = J'' = 32$ line) determined by the above method amounted to 0.039 ± 0.003 at $3059^{\circ}K$, the highest temperature at which intensities were measured. The size of this quantity justifies the assumptions involved in using the approximations (31) and (32). From this value the values of $\underline{R_0}$ at lower temperatures were calculated by the use of the measured temperature coefficients for the intensity of the Phillips rotational line and Wien's law to correct the measured black-body intensity to other temperatures. To simplify this procedure it was assumed that $\Delta\nu_D$ is constant, which is a good approximation considering that the temperature range, 300° to 400°, is small compared with the absolute temperature; $\Delta\nu_D$ varies only as the square root of the temperature as shown in Eq. (36). The R_0 values and the corresponding correction factors thus calculated for this particular Phillips rotational line are presented in Table VI for a number of temperatures in the range in which intensities were measured. Now we may see that the uncertainty quoted for the measured $\underline{R_0}$ amounts to an uncertainty in the correction factor of only one in a thousand at the highest temperature.

Table VI

Self-absorption correction factors for Phillips (2-0) band, $J' = J'' = 32$ line, at different tempertures

T (^oK)	$R_0 \times 10^2$	Q
3100	6.03	1.021
3000	2.07	1.007
2900	.658	1.002
2800	.194	1.001
2700	.0519	1.0002
2600	.0257	1.0001

D. Self-Absorption in the (0-0) and (1-0) Swan-Band Heads

The application of self-absorption corrections to the Swan bands is more complicated than in the case of the single Phillips rotational line. Here we must look at the head of a band composed of many Doppler-broadened rotational lines all spaced very closely together. We may consider three possible cases. In the first the rotational lines are so closely spaced that the lines are completely unresolvable even with a spectrograph of infinite resolving power, i.e., where the peaks of each two adjacent lines are within the Doppler width of each other. This is the simpler case, since we may then regard the band head as a continuum; thus if the slits of the spectrograph are narrow compared with the width of the band head, the correction factors may be calculated quite accurately from the monochromatic Eq. (28) or (32). The R_ν values would be determined experimentally in a manner similar to that used for the Phillips line, except that here, of course, there would be no need to correct for instrumental broadening.

In the second case all the rotational lines are spaced far enough apart that they could be resolved by a spectrograph of infinite resolving

power, i.e., where no two adjacent lines are as close as the Doppler half width, yet where an ordinary spectrograph with wide slit widths sees the resolvable rotational lines as a continuous band head. Here one can calculate the intensities of the individual rotational lines that contribute to the band head if one knows the intensity of the instrumentally recorded band head. From these intensities correction factors can be calculated for each individual rotational line by the procedure given in previous paragraphs on the Doppler-broadened line. The total correction factor for the instrumentally recorded band head can then be calculated by averaging the individual correction factors for each line and weighting each one according to the contribution that particular rotational line makes to the instrumentally recorded band head.

The third case is a compromise between the first two cases; where some of the individual rotational lines that make up the band head are resolvable and some not resolvable by a spectrograph of infinite resolving power. In this case the head is composed of individual lines and groups of unresolvable lines as viewed through an instrument of infinite resolving power. It may be pointed out that for a given band head whose intensity has been measured one will obtain the largest self-absorption correction if one assumes that it is an example of Case Two, the next largest if one assumes Case Three, and the smallest for Case One.

It was found that the Swan bands fell in Case Three. Phillips[29] calculated the positions of the components of the triply split rotational lines of the (0-0) vibrational band of the Swan system, using the formulas of Budo.[4] The positions of the triplet components in the P branch, which forms the head of the (0-0) band, are such that there are groups of lines that are closer in spacing than the Doppler width calculated for these lines at the temperatures of the intensity measurements.

The procedure used in this case to evaluate the correction factors for the Swan (0-0) and (1-0) bands was as follows. The positions calculated by Phillips for the components of the P branch of the (0-0) band, were used for making a plot of the intensity of the triplet components versus frequency; triangles were used that had a Doppler half

width and heights proportional to the calculated intensities of these lines.* The intensities of these lines were then summed up at equal frequency intervals; thus was obtained the profile of the band head as it would look when observed by an instrument of infinite resolving power.

This profile is presented in Fig. 9, and shows a number of peaks corresponding to individual lines and to groups of lines with valleys in between the groups occasionally dropping to zero intensity. The ratio of the intensities of these peaks to the intensity of the instrumentally recorded band head was determined by dividing the profile into sections and calculating what each of these sections contributed to the particular frequency where the instrumental maximum intensity was recorded. This contribution was proportional to the relative integrated intensity of the particular section, and decreased as the distance of the section from the frequency of the maximum recorded intensity increased. A slit width had to be assumed for the instrument, because sections of the profile farther than one slit width from the frequency of maximum intensity contributed nothing to the instrumentally recorded maximum intensity. A slit width was chosen that gave a calculated profile for the instrumentally recorded band head closest to that actually obtained on the recording when the feature was traced by the instrument. This instrumental maximum is indicated in Fig. 9 by the dotted line, which has the shape of the instrumentally recorded feature and is plotted using the same arbitrary intensity scale as the completely resolved profile.

When the ratios of the intensities of the different sections of the profile to the measured intensities had been calculated, the $\underline{R}$ values at all wavelengths along the infinitely resolved profile could be calculated; the ratio of the instrumental maximum intensity to the intensity of a black body had been determined in a manner similar to that used for the Phillips rotational line. Then, by means of Eq. (28) the correction factors could be calculated at any of these frequencies.

---

*To simplify calculations, the same distribution of rotational lines in the head was assumed for the Swan (1-0) band as for the (0-0) band.

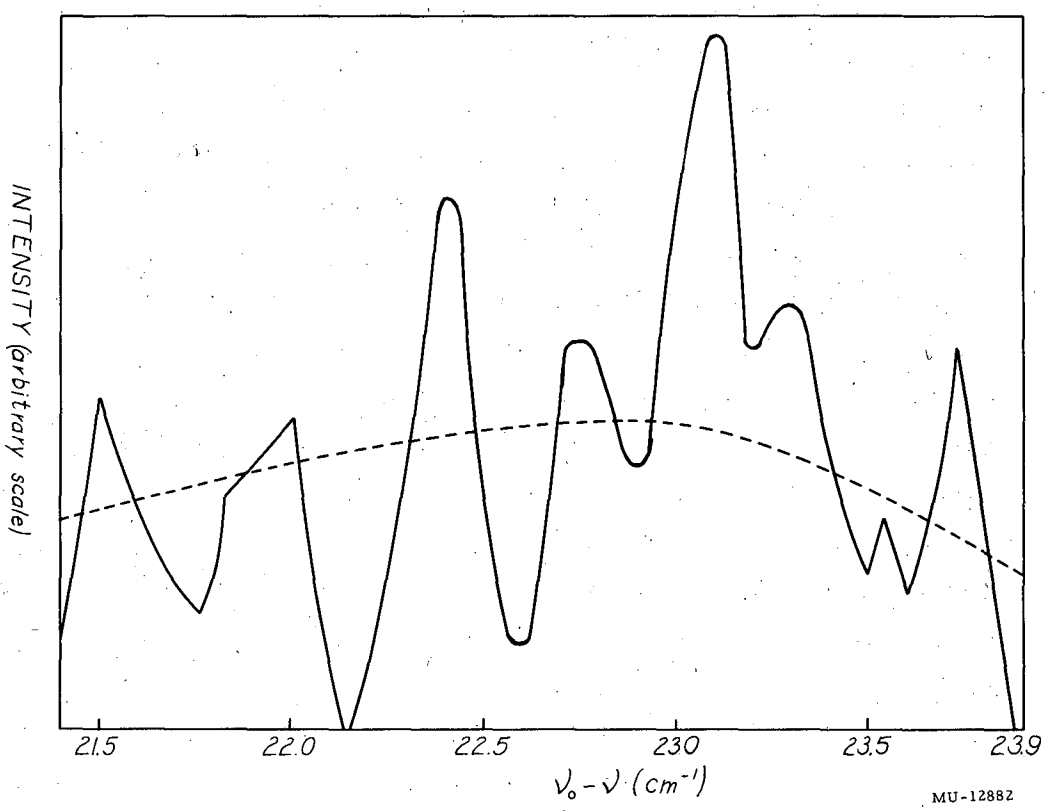

Fig. 9. Infinitely resolved profile of Swan (0-0) band head (solid line). Dotted line represents profile of instrumental recording. ν_0 is frequency of origin of band in cm^{-1}.

These correction factors were integrated over the sections of the profile by use of Eq. (29) and substitution of Eq. (28) or (32) for $\underline{Q}$ in this equation. From these integral correction factors the correction factor for the instrumental peak intensity could be calculated; the correction factors of the different sections that contributed to the instrumental peak were averaged, with each factor weighted according to the contribution that particular group made to the instrumental peak. If this correction factor turned out to be appreciable, then it was necessary to assume correction factors for each section and for the instrumental peak when finding their contribution to the instrumental peak, since these contributions were originally calculated on assumption of no self-absorption. Then the correction factors were calculated and used as a second approximation, and the process repeated until the assumed and calculated factors agreed. The correction factor for the instrumental peak was determined at other temperatures in the same manner; the calculations were simplified by assuming that the relative intensities of the different rotational lines contributing to the head did not change over this comparatively small temperature range.

The value measured for the ratio of instrumental peak intensity to intensity of a black body at the same temperature as the column of gas was 0.185 ± 0.012 at a temperature of $3007^{\circ}K$ for the Swan (0-0) band head and 0.061 ± 0.004 at $2997^{\circ}K$ for the Swan (1-0) band. For the (1-0) band the ratio was measured in the first order of the 3-meter grating with slits varying from 0.025 to 0.10 mm, corresponding to 0.05 to 0.20 mm in the second order; there was no significant variation in the ratio thus obtained. This indicates that the slit widths were narrow compared with the effective width of the feature. These ratios were calculated at other temperatures by use of the observed variation in intensity of the bands with temperature, and of Wien's law to correct the black-body intensity. When these ratios were measured at other temperatures, the values obtained agreed with the above values within the quoted uncertainty. From these values of $\underline{R}$, values of $\underline{Q}$, the correction factor, were calculated by the methods of Case Three. These values are presented in Table VII along with values of $\underline{Q}$ calculated by

the methods of Case One for comparison. It will be noted that the methods of Case One and Case Three lead to the same values of Q when low values of R are used. This is because Q varies linearly with R in this region; therefore the high values of Q possessed by the parts of the infinitely resolved profile represented in Fig. 9 that are above the instrumentally recorded profile are just balanced out by the parts of the infinitely resolved profile that are below that of the instrument. The Case Three correction factors were the ones actually used in calculating the heats.

Table VII

Self-absorption correction factors calculated for the Swan (0-0) and (1-0) band heads by the method of both Case One and Case Three

T (°K)	Swan (0-0) band			Swan (1-0) band		
	R	Q(Case 1)	Q(Case 3)	R	Q(Case 1)	Q(Case 3)
3100	0.418	1.294	1.334	0.171	1.097	1.100
3000	0.175	1.098	1.103	0.0627	1.039	1.039
2900	0.0616	1.040	1.040	0.0213	1.011	1.011
2800	0.0199	1.010	1.010	0.00673	1.003	1.003
2700	0.00574	1.003	1.003	0.00194	1.001	1.001
2600	0.00151	1.001	1.001	0.000512	1.0003	1.0003

Relative f values for the Swan (0-0) and (1-0) bands may be obtained from Table VII by multiplying the R values of the (0-0) and (1-0) heads by their respective correction factors.* In this manner we find that the f value of the (0-0) band is 2.97 times that of the (1-0) band. This value should have a much smaller uncertainty than those quoted above for a particular R value measured under widely different conditions.

*From Eq. (25) and (26) we obtain $Q_\nu R_\nu = b_\nu NL$, where N is the concentration of molecules in the lower state of the transition. This quantity is proportional to the f value for the transition.

This is because the two $\underline{R}$ values were measured with the same heating tube at almost the same time. Thus errors in path length and temperature measurement were cancelled out, and the relative values of the two $\underline{R}$'s should be known quite accurately. This value of 2.97 may be compared with a value calculated by Fraser, Jarman and Nicholls[10] of 3.08 or King's[17] measured value of 2.79.

Because the correction factors were smaller for the Swan (1-0) band head, it was felt that more accurate heats would be obtained if this band were used for the final determination of the heats. Under the conditions of the intensity-measuring experiments the intensity of the Swan (1-0) band was of the same order of magnitude as the intensity recorded for the Phillips rotational line, and therefore using a band of higher intensity would not have appreciably increased the accuracy with which the intensities could be measured.

The cause of part of the discrepancy between the two values for the heat of sublimation of C_2 found in Krikarian's work and this work may lie in the self-absorption corrections. Krikorian's self-absorption corrections added 11.9 kcal to his heat of formation of Zr and 7.2 kcal to his heat of sublimation of C_2. These self-absorption corrections for the Swan (1-0) band head lead to values of the ratio of the intensity of the band head to a black body at the same temperature that are two to five times the size of these ratios found in this experiment, when compared at the same temperatures and on the same temperature scale. Furthermore, the temperature coefficient of the ratios he used disagrees with the heat he obtained for the formation of the particular level responsible for the emission. The ratios of intensities measured in this work lead to relative $\underline{f}$ values for the (0-0) and (1-0) Swan bands which agree well with those measured and calculated by other observers; furthermore, his ratios lead to absolute $\underline{f}$ values for these bands that are four to ten times those measured by King. Thus it is felt that Krikorian's ratios are considerably too high. Krikorian measured the ratios of the intensities of his features to that of a black body in a manner similar to that used in this work. The larger values which he thus obtained for these ratios may be explained by the possibility that

he used nonequivalent optics when comparing the two intensities. For example, he may not have observed equivalent areas of the two sources, or possibly in his measurement not all the light passing through the slit fell on the diffraction grating. Therefore the self-absorption corrections and consequently the heats in Krikorian's work were adjusted to agree with the self-absorption corrections used in this work. Such corrections were not determined in this work for the Zr feature; it was assumed, however, that the ratio measured by Krikorian for the intensity of this feature to the intensity of a black body at the same temperature is in error by the same factor as for the Swan (1-0) band head. One can then obtain corrections for both his Zr heat of formation and the sublimation heat of C_2 that will make their self-absorption contributions more consistent with the work reported here.

In this manner one finds that Krikorian's Zr heat should be lowered by 6.8 kcal and his C_2 heat by 4.1 kcal. Thus the value which he quotes for the heat of sublimation of C_2 should be raised by the difference in these corrections; he obtained this value by measuring the difference in energy between the emitting levels of Zr and C_2 and subtracting this value from the heat of formation of the excited state of Zr.

E. Limiting Slope of Curves for Heat vs. Scanning Speed

In order to extrapolate the curves of Figs. 5, 6, and 7 to the ordinate, the nature of the limiting slope of the curves had to be determined. According to Krikorian[19] the peak intensity of a triangularly shaped feature recorded with scanning speed s is given by the formula

$$I_s = I_0 \left[1 - \frac{st}{\Delta\lambda} \ln \left(2 - e^{-\Delta\lambda/st} \right) \right] . \qquad (37)$$

Here I_0 is the true peak intensity of the feature; t is the time constant for the amplifier and Cs_2O cell circuit, and varies with the stage of amplification used; $\Delta\lambda$ is the half width of the instrumentally broadened feature. The Cs_2O cell and amplifier should obey this formula, since their response is limited principally by the charging or discharging of a condenser across a resistance in the feedback circuit, which is the assumption on which this formula is based.

Using this formula, we may arrive at an expression for the limiting slope of plots of ΔH^o_{3000} against s; ΔH^o_0 will have the same limiting slope because it differs from ΔH^o_{3000} by only a constant term. For the points at the ends of the sigma plots we may say

$$\Delta H^o_{3000} = \frac{\Sigma' - \Sigma''}{(1/T'' \quad 1/T')} = \frac{R}{\Delta(1/T)} \ln \frac{I'_s T'}{I''_s T''} . \qquad (38)$$

The prime represents points taken at the highest temperature, and the double prime indicates the lowest temperature. At the lowest scanning speed used in this experiment the exponential term in Eq. (37) is negligible, and we may substitute $I_s = I_0 (1 - Cs)$ into Eq. (38); C is equal to $t \ln 2/\Delta\lambda$ and depends as t does on the particular gain of amplification being used. We may obtain the slope at low scanning speeds for the curves by differentiating Eq. (38) with respect to s:

$$\frac{d(\Delta H^o_{3000})}{ds} = \frac{R}{\Delta(1/T)} \left(\frac{C''}{1-C''s} - \frac{C'}{1-C's}\right) . \qquad (39)$$

With values of s ranging from zero to the lowest scanning speed used here, the limiting slope is almost constant, and is given by

$$\frac{d(\Delta H^o_{3000})}{ds} = \frac{R}{\Delta(1/T)} (C'' - C') = \frac{R \ln 2}{\Delta\lambda\Delta(1/T)} (t'' - t'). \qquad (40)$$

On this basis the curves of Figs. 5, 6, and 7 should be extrapolated to the ordinate by drawing straight lines tangent to the curves at the points measured at the lowest scanning speed.

Through the use of Eq. (40) the limiting slopes of Figs. 5, 6, and 7 may be computed. The values thus obtained agreed with the limiting slopes of the curves within the accuracy with which the time constants of the circuit could be determined.

REFERENCES

1. L. Brewer, P.W. Gilles and F.A. Jenkins, J. Chem. Phys. 16, 797 (1948).
2. L. Brewer and J.G. Phillips, unpublished work.
3. L. Brewer and A.W. Searcy, Annual Reviews of Physical Chemistry, H. Eyring, ed., Annual Reviews Inc., Palo Alto, 1956, Vol. 7, p. 271.
4. A. Budó, Z. Physik 96, 219 (1935); 98, 437 (1936).
5. W.A. Chupka and M.G. Inghram, J. Phys. Chem. 59, 100 (1955).
6. R.J. Corruccini, J. of Res. of NBS. 43,133 (1949).
7. W. de Sorbo, J. Am. Chem. Soc. 77, 4713-5 (1955).
8. J.C. de Vos, Physica 20, 690 (1954).
9. W.E. Forsythe, "Optical Pyrometry", Temperature Its Measurement and Control in Science and Industry, Amer. Inst. of Physics, Reinhold, New York, 1941, p. 1115.
10. P.A. Fraser, W.R. Jarman and W. Nicholls, Astrophys. J. 119 (1954).
11. H. Freymark, Ann. Physik 8, 221 (1951).
12. A.G. Gaydon, Dissociation Energies and Spectra of Diatomic Molecules, 2nd ed., Chapman and Hall, London, 1953.
13. A.R. Gordon, J. Chem. Phys. 5, 350 (1937).
14. G. Herzberg, Molecular Spectra and Molecular Structure, I. Spectra of Diatomic Molecules, 2nd. ed., Van Nostrand, New York, 1950.
15. R.E. Honig, J. Chem. Phys. 22, 126 (1954).
16. K.K. Kelley, U.S. Bur. Mines Bull. 383, 31 (1935).
17. R.B. King, Astrophys. J. 108, 429-33 (1948).
18. R.B. King, private communication with L. Brewer.
19. O.H. Krikorian, "High Temperature Studies: III. Heat of Formation of the $^3\Pi_u$ State of C_2 from Graphite", University of California Radiation Laboratory Report No. UCRL-2888, April, 1955.

20. H.G. Mac Pherson, J. Opt. Soc. Amer. 30, 189 (1940).
21. A.C.G. Mitchell and M.W. Zemansky, Resonance Radiation and Excited Atoms, Cambridge, University Press, London, 1934, p. 96-7.
22. C.E. Moore, A Multiplet Table of Astrophysical Interest, Part II: Finding List, Contributions from the Princeton University Observatory, No. 20, 1945.
23. C.E. Moore, Atomic Energy Levels, Vol. I, U.S. National Bureau of Standards Circular 467, June 15, 1949.
24. R.S. Mulliken, Phys. Rev. 56, 778 (1939).
25. J.G. Phillips, Astrophys. J. 107, 389 (1948).
26. J.G. Phillips, Astrophys. J. 108, 434 (1948).
27. J.G. Phillips, Astrophys. J. 119, 274 (1954).
28. J.G. Phillips, and L. Brewer, Société Royale des Sciences de Liège Mémoires, Quatrième Série, Tome XV, 341-51, (1955).
29. J.G. Phillips, private communication, 1956.
30. Ned Rasor, Wright Air Development Center, Report No. WADC TR 56-400, Part I, 1956.
31. B. Rosen, Constantes Sélectionnées, Données Spectroscopiques, Hermann, and Co., Paris, 1951; Constantes Sélectionnées, Atlas, Hermann, Paris, 1952.
32. F.D. Rossini, D. Wagman, W. Evans, S. Levine and I. Jaffe, Selected Values of Chemical Thermodynamic Properties, Series III, U.S. Bureau of Standards, 1948.
33. H. Shull, Astrophys. J. 112, 352-60, (1950).
34. G. Stephenson, Proc. Phys. Soc. 64A, 99 (1951).
35. D.R. Stull and G.C. Sinke, Thermodynamic Properties of the Elements, Advances in Chemistry Series, No. 18, American Chemical Society, Washington, 1956, p. 69.
36. R.J. Thorn and G.H. Winslow, J. Chem. Phys. 26, 186 (1957).